TECHNICAL REPORT BRL-TR-3023

BRL

THE MECHANICAL RESPONSE OF M30, JA2 AND XM39 GUN PROPELLANTS TO HIGH-RATE DEFORMATION

ROBERT J. LIEB

AUGUST 1989

U.S. ARMY LABORATORY COMMAND

BALLISTIC RESEARCH LABORATORY
ABERDEEN PROVING GROUND, MARYLAND

UNCLASSIFIED

SECURITY CLASSIFICATION OF THIS PAGE

REPORT DOCUMENTATION PAGE

Form Approved OMB No. 0704-0188

1a. REPORT SECURITY CLASSIFICATION Unclassified	1b. RESTRICTIVE MARKINGS
2a. SECURITY CLASSIFICATION AUTHORITY	3. DISTRIBUTION/AVAILABILITY OF REPORT APPROVED FOR PUBLIC RELEASE; DISTRIBUTION UNLIMITED
2b. DECLASSIFICATION/DOWNGRADING SCHEDULE	
4. PERFORMING ORGANIZATION REPORT NUMBER(S) BRL-TR-3023	5. MONITORING ORGANIZATION REPORT NUMBER(S)
6a. NAME OF PERFORMING ORGANIZATION US Army Ballistic Research Lab 6b. OFFICE SYMBOL (If applicable) SLCBR-IB-P	7a. NAME OF MONITORING ORGANIZATION
6c. ADDRESS (City, State, and ZIP Code) Aberdeen Proving Ground, MD 21005-5066	7b. ADDRESS (City, State, and ZIP Code)
8a. NAME OF FUNDING/SPONSORING ORGANIZATION 8b. OFFICE SYMBOL (If applicable)	9. PROCUREMENT INSTRUMENT IDENTIFICATION NUMBER
8c. ADDRESS (City, State, and ZIP Code)	10. SOURCE OF FUNDING NUMBERS PROGRAM ELEMENT NO. / PROJECT NO. / TASK NO. / WORK UNIT ACCESSION NO.

11. TITLE (Include Security Classification)
THE MECHANICAL RESPONSE OF M30, JA2 AND XM39 GUN PROPELLANTS TO HIGH RATE DEFORMATION

12. PERSONAL AUTHOR(S)
Robert J. Lieb

13a. TYPE OF REPORT	13b. TIME COVERED	14. DATE OF REPORT (Year, Month, Day)	15. PAGE COUNT
TR	FROM Jun 84 TO Dec 88		

16. SUPPLEMENTARY NOTATION

7

17. COSATI CODES			18. SUBJECT TERMS (Continue on reverse if necessary and identify by block number)
FIELD	GROUP	SUB-GROUP	Gun Propellant, High Rate Testing, Mechanical Properties, IB Codes, Fracture Damage, M30, JA2, XM39

19. ABSTRACT (Continue on reverse if necessary and identify by block number)

The high rate mechanical properties measurements of M30, JA2 and XM39 gun propellants that have been gathered over the past several years, and the procedure by which these data were gathered and analyzed are documented in this report. The conditions under which the tests have been performed encompass the temperature range of ballistic interest, include strain rates from static to 10,000/s, and cover regions of pressure from atmospheric to 400 MPa. These results are presented and analyzed to show the nature of the mechanical response changes. Constitutive relationships were extracted from these results and are presented. These equations that may be used as a initial attempt to predict the interior ballistic mechanical response under operational conditions.

Appendices contain the data acquisition and reduction program, the uniaxial compressive gun propellant test procedure, and an illustration explaining the measured parameters.

20. DISTRIBUTION/AVAILABILITY OF ABSTRACT	21. ABSTRACT SECURITY CLASSIFICATION
☐ UNCLASSIFIED/UNLIMITED ☒ SAME AS RPT ☐ DTIC USERS	UNCLASSIFIED

22a. NAME OF RESPONSIBLE INDIVIDUAL	22b. TELEPHONE (Include Area Code)	22c. OFFICE SYMBOL
ROBERT J. LIEB	(301)278-6195	SLCBR-IB-P

DD Form 1473, JUN 86 Previous editions are obsolete

SECURITY CLASSIFICATION OF THIS PAGE

UNCLASSIFIED

TABLE OF CONTENTS

LIST OF ILLUSTRATIONS

I. INTRODUCTION

The mechanical response of gun propellant to high rate deformation plays a critical role in the performance of guns and in the violence of the response of the propellant to vulnerability threats. However, unlike engineering materials, which have most of their critical characterizations performed within a range of state from stress-free up to conditions of failure, propellant performance is most affected by mechanical response only after failure has occurred. Indeed, the changes in propellant dimensions, under ideal firing conditions where no failure occurs, have been shown using a ballistic code to have almost no effect on gun performance. Propellant performance within an established charge depends on the rate of generation of gases through combustion (mass generation rate). This mass generation rate of the propellant depends on the its burning rate, density, and the total surface area undergoing combustion. This relationship can be expressed by the following:

$$dm/dt = \rho r A \quad (1)$$

where dm/dt is the mass generation rate, ρ is the mass density, r is the pressure dependent burning rate, and A is the exposed surface area. The variable critically influenced by the mechanical response is A.

Until propellant failure conditions exist within the gun, A is a well controlled parameter. Unprogramed generation of surface area can come from several sources. If individual grains are projected against interior surfaces, such as cartridge case walls, the projectile base, or protruding projectile fins, single grain impact results. The fracture generated surface area of the grain will depend on factors such as the impact velocity, orientation, and temperature of the grain. Grain-grain interaction is also possible and has been described as an intergranular stress wave propagating through the bed. If this stress state exceeds critical limits, fracture surface area will be generated. A third failure mechanism results when the pressure differences between the gun chamber and the grain perforation exceed critical values. This pressure difference can be positive, if the perforation pressure of ignited grains exceed ambient pressures,[1,2] or negative, if the ambient pressure exceeded the perforation pressure as could be the case in an unignited grain within an ignited bed. This results in the grain or stick bursting or collapsing, and unprogramed surface area being added during the combustion process. The propellant susceptibility to fracture can be evaluated by measuring changes in the propellant mechanical response. If the propellant is properly characterized, this susceptibility can be compared to acceptable performers or used to point out response characteristics that need to be changed to enhance performance.

Until recently, only low rate mechanical response measurements were made on these materials. Since most propellants are polymeric systems that may or may not be filled, the response is sensitive to the rate of testing. However, methods were developed for a standardized high rate compressive measurement technique some years ago. These measurement techniques[3,4] were performed on M30, JA2, and XM39 gun propellants at strain rates on the order of 200 per second over the entire temperature range of ballistic interest. These are rate conditions that more closely resemble the operational environment. This report describes the technique and the results of many mechanical properties measurements taken over the past few years. Also included are high rate, high pressure results performed at Lawrence Livermore National Laboratory (LLNL).

II. EXPERIMENTAL METHOD

A. The Apparatus

The machine used to measure the high rate response is the Drop Weight Mechanical Properties Tester (DWMPT) and is illustrated in Figure 1. This device was calibrated[3] using aluminum cylinders, and found to provide modulus measurements within 9% of the handbook values with a 5 % standard deviation. The relative softness of gun propellant (E(p) = 5 GPa vs E(Al) = 72 GPa) will favor more accurate measurements when used for propellant. The principle of operation is as follows. The falling weight cage transmits the high rate impulse through the ram to the specimen. The ram is also used to measure the specimen displacement by optically tracking the change in location of the specimen (illustrated in Figure 2). The impulse acts upon the specimen and is measured utilizing the force gage located directly beneath the specimen.

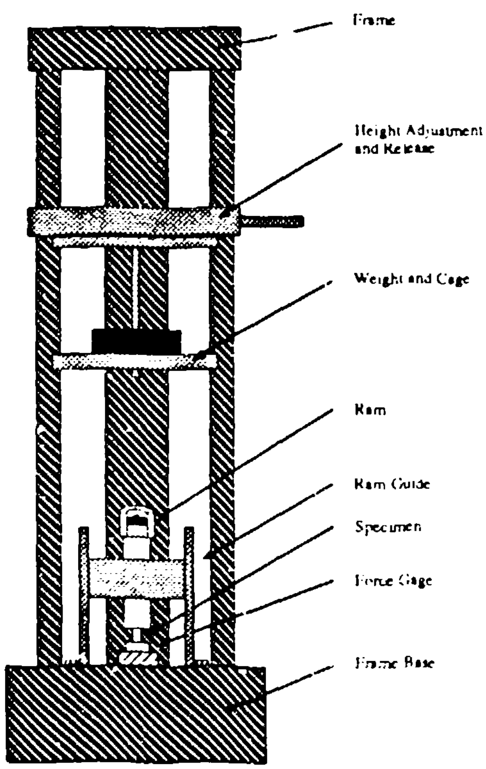

Figure 1. The Drop Weight Mechanical Properties Tester

The nature of the impulse can be changed by adjusting the total mass (drop weight) and distance (drop height) through which this mass falls before hitting the ram. The total energy available is increased by increasing either of these, but the strain rate is principally dependent on the drop height and almost independent of the drop weight. This permits the impact energy to be adjusted with some independence from the strain rate.

Low temperature conditioning is accomplished by enclosing the ram, ram guide, force gage, within a copper shell through which liquid nitrogen vapor is circulated. This shell is illustrated in Figure 3, and is able to keep the specimen conditioned to within one degree Celsius of the desired temperature. Temperature differences within the chamber are usually kept under one degree, although at the extreme low temperatures, heat fluxes through the ram and base are thought to disrupt the temperature uniformity. Higher than ambient temperatures are obtained by wrapping this shell with a heating strip. Temperatures up to 63°C can be obtained with a two degree maximum temperature difference within the chamber.

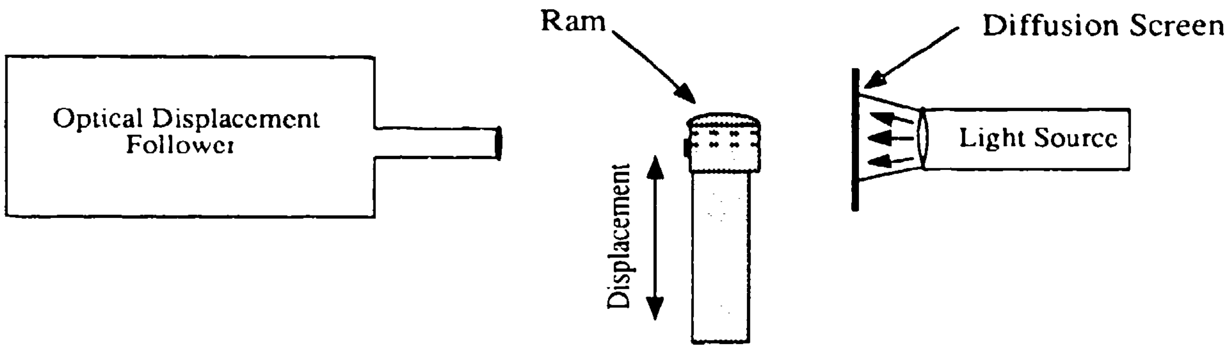

Figure 2. Illustration of the DWMPT Optical Displacement Measurement Technique

B. The Specimen and Specimen Conditioning

Specimens are cut from granular or stick propellant with a diamond saw. Since the length to diameter ratio (L/D) for most granular propellant usually lies between 1.1 and 1.5, a standard specimen length was chosen to have a L/D ratio of 1.00 ± 0.05. This should reduce the influence of differential end effects for propellants of the same type but having different dimensions. The cut surfaces are parallel to each other to within 0.1 degree and each surface is perpendicular to the cylinder axis to within 0.5 degree. All physical dimensions are measured to within 0.01 mm. An illustration of a seven-perforated specimen appears as shown in Figure 4.

Specimen temperature conditioning is done within a temperature-conditioning copper chamber which keeps the ambient temperature of the grain controlled to within 1°C. The specimens are conditioned for a period that is sufficiently long (depending on grain size) to ensure that uniform temperatures are attained. Transfer of the specimen into conditioned equipment takes place in less than 10 seconds. Time is then allotted for the specimen to recover from any thermal disruption that may have occurred due to the transfer.

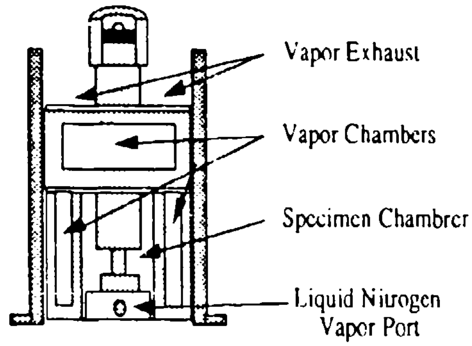

Figure 3. DWMPT Temperature Conditioning Shell

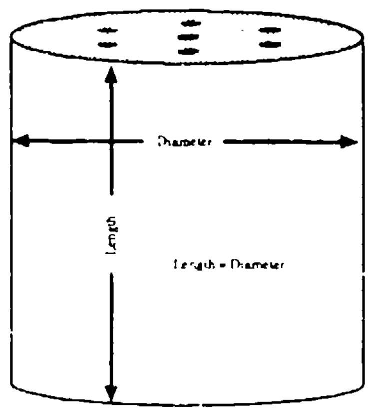

Figure 4. Illustration of a Seven-Perforated Test Specimen

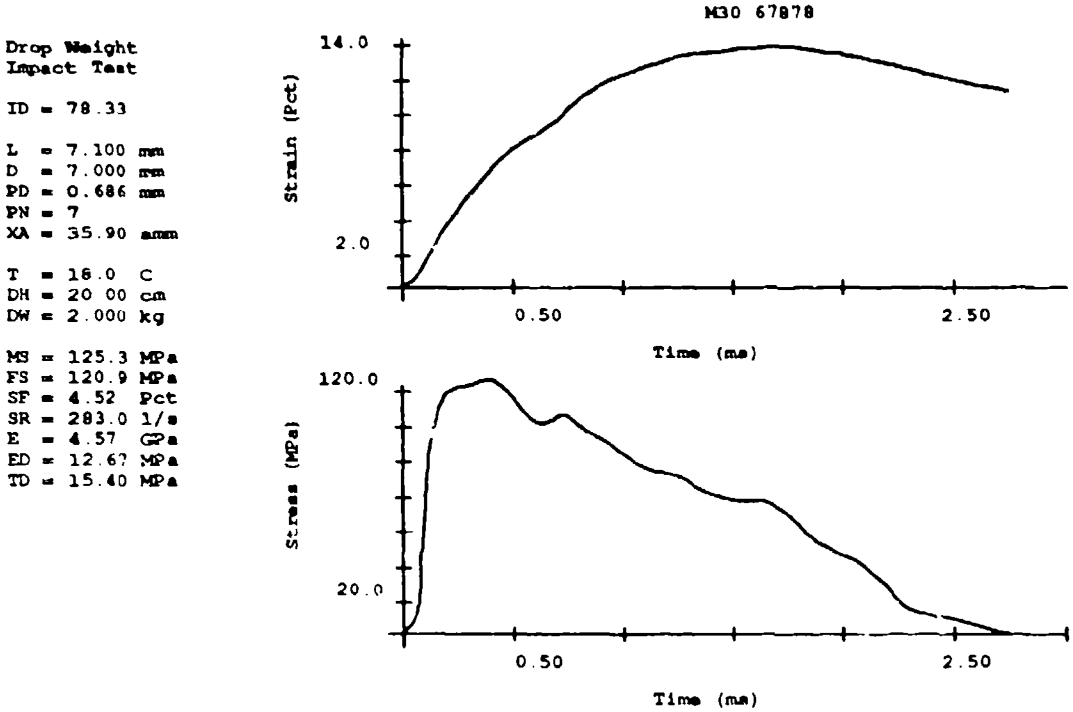

Figure 5. Graphic Output from the High Rate Mechanical Response Data Acquisition Program

C. The Procedure

Prepared specimens are tested to failure at a given strain rate by selecting the appropriate drop height and weight. Once the conditions of the test are determined and attained, the weight cage is released and data acquisition of the high rate event proceeds. The raw, 2-channel event information is digitized and recorded on disk as displacement and force gage voltage signals. Test conditions, data identification number, specimen dimensions, and other test information are also recorded. The data are transformed into stress and strain records, using the above information, with gage temperature corrections, tester compliance compensation, and calibration coefficients being utilized. An example of the graphic output is provided in Figure 5. Appendix A contains the documentation and an annotated listing of the program used in the acquisition and analysis of these data.

Information listed on the output is as follows: The Maximum Stress (MS) is the highest stress level achieved, the Stress at Failure (FS) is the stress at yield, the Strain at Failure (SF) is the strain corresponding the Stress at Failure, the Strain Rate (SR) is rate of compressive deformation taking place before failure, the Modulus (E) is the slope of the linear portion of the Stress vs Strain plot, the Impact Energy Density (ED) is the value of the integral of the Stress vs Strain over the entire event, i.e. the absorbed energy density, and the Theoretical Energy Density (TD) is the total gravitational potential energy of the weight cage able to be delivered to the grain divided by the initial grain volume. The procedure[5] followed and the definitions of

Table 1. Percent Composition of JA2, M30, and XM39 Gun Propellants

Component	JA2	M30	Component	XM39
Nitrocellulose	59	28	RDX (Ground)	76.0
NC Nitration Level	13.0	12.6	Cellulose Acetate Butyrate	12.0
Nitroglycerin	15	22	Acetyl Triethyl Citrate	7.6
Nitroguanidine	0	48	Nitrocellulose	4.0
Ethyl Centralite	0	2	NC Nitration Level	12.6
Diethylene Glycol Dinitrate	25	0	Ethyl Centralite	0.4
Akardit II	1	0		

the terms listed above appear in Appendix B. Appendix C illustrates how these measurements are determined.

The above quantities were measured for M30, JA2, and XM39 in a series of experiments that spanned several years. M30 and JA2 are conventional tank gun propellants. M30 is a triple base formulation and JA2 is a double base. XM39 is a Low Vulnerability Ammunition (LOVA) formulation designed to reduce the system vulnerability to the ignition of stowed propellant that may result from armor piercing spall or direct projectile interaction. Each of these propellants has significant mechanical response differences which help to elucidate the problem of characterizing important properties. The chemical composition of these propellants is found in Table 1. Figures 6 through 8 show the Stress vs Strain for each of these propellants at several temperatures over the range of ballistic interest. The curves appearing in these plots represent the average values of at least five tests, and show the response of the propellant to high rate deformation.

III. RESULTS AND ANALYSIS

A. Significant Parameters

The information most used in the characterization of the mechanical response of the propellant is the Stress at Failure, Strain at Failure, and Modulus. The changes in these quantities with corresponding changes of an independent variable (such as temperature, pressure, or percent composition) provide insight into the response changes that can be expected. For example, if the Stress at Failure increases dramatically as the temperature is lowered, and the Strain at Failure has a corresponding decrease, a transition toward brittle behavior is likely to have occurred. Such trends are often not so simply observed. How these mechanical properties change with formulation or processing changes is an important consideration that affects the evaluation of fracture susceptibility and continues to undergo active investigation and development.

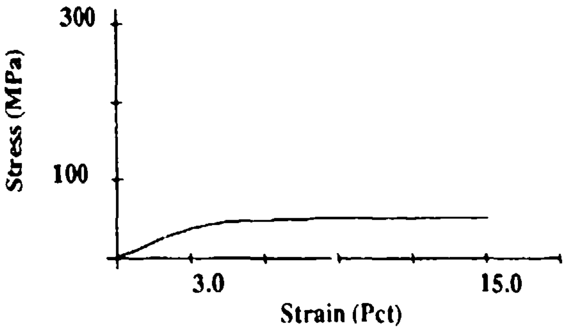

a. 60°C

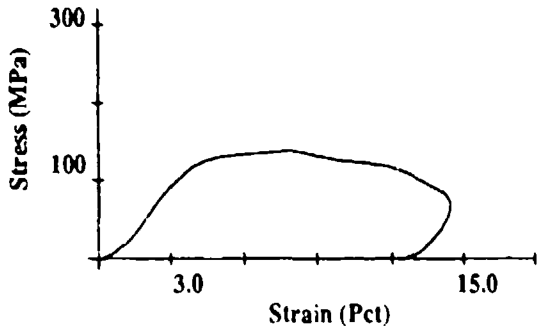

b. 18°C

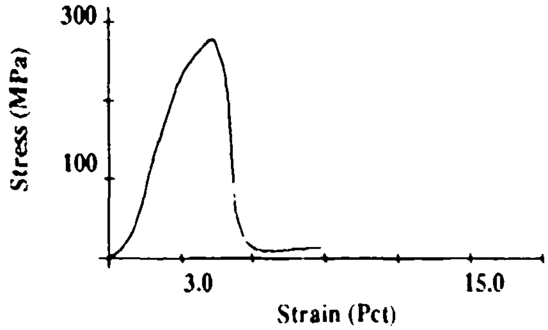

c. -40°C

Figure 6. Stress vs Strain for M30 Propellant at Strain Rates of about 250 s^{-1}

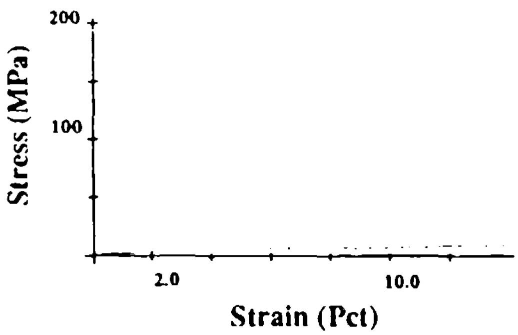

a. 60°C

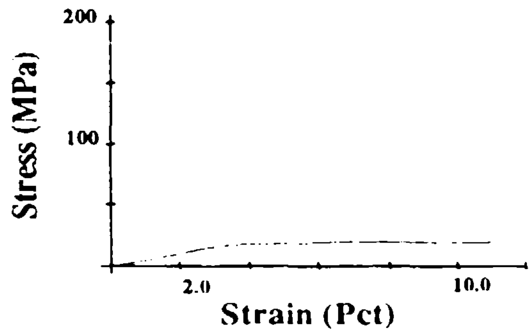

a. 20°C

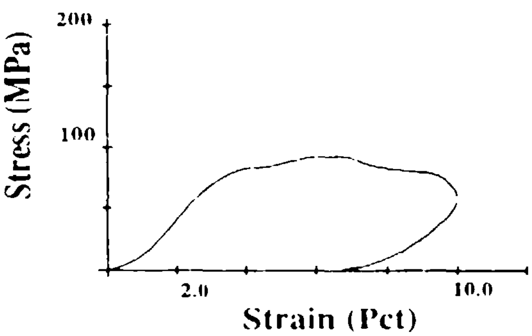

a. -20°C

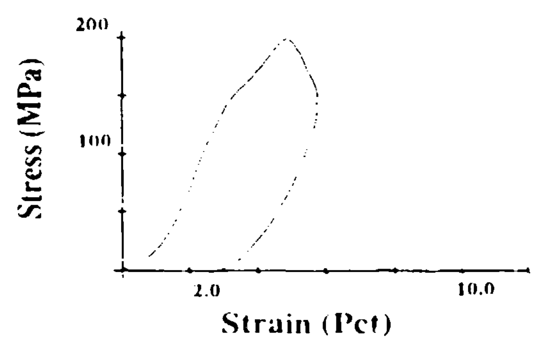

a. -40°C

Figure 7. Stress vs Strain for JA2 Propellant at Strain Rates of about 250 s^{-1}

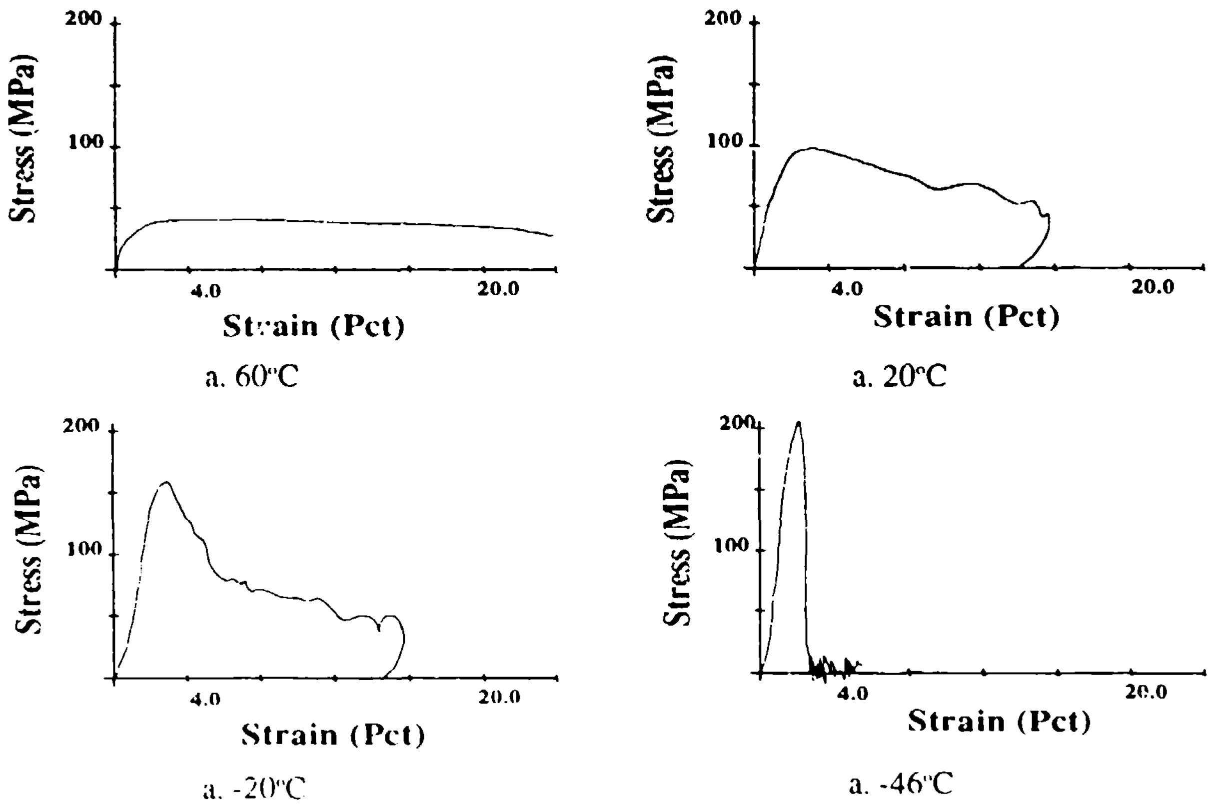

Figure 8. Stress vs Strain for XM39 Propellant at Strain Rates of about 250 s^{-1}

It can be seen, from the information presented in Appendix C, that the stress at failure and the corresponding strain are difficult to define in some cases. For a very brittle response the choice of a failure point is somewhat easier. There is a quick break from linearity and a dramatic loss of specimen strength, as for XM39 at -46 °C or even -20 °C. For very plastic responses, as in the case of JA2 at temperatures above -20 °C, the choice is not difficult either. Once flow begins the stress level remains about constant, so the stress level required for plastic flow can be determined. The difficult case occurs when flow and fracture occur together.

Since these materials are not structural, deviations from linear response are not of paramount importance. What is important is the ability of the propellant to resist significant increases in fracture generated surface area. Large increases only occur after failure. This means that traditional yield stresses may not be an important measurement. A question such as "What stresses can the propellant withstand before it undergoes significant changes in surface area?" becomes important. It is clear from the response of M30 propellant and the closed bomb analysis done on tested grains[6] that significant increases in surface area do not occur at the yield point. It is beyond this point that significant increases occur. The problem of defining a meaningful failure point for propellants not exhibiting either brittle or plastic behavior is difficult to address.

The method used to define failure in these studies takes into consideration the ideas outlined above. Figure 9 shows the Stress vs Strain curve for M30 at 18 °C. This is a typical curve

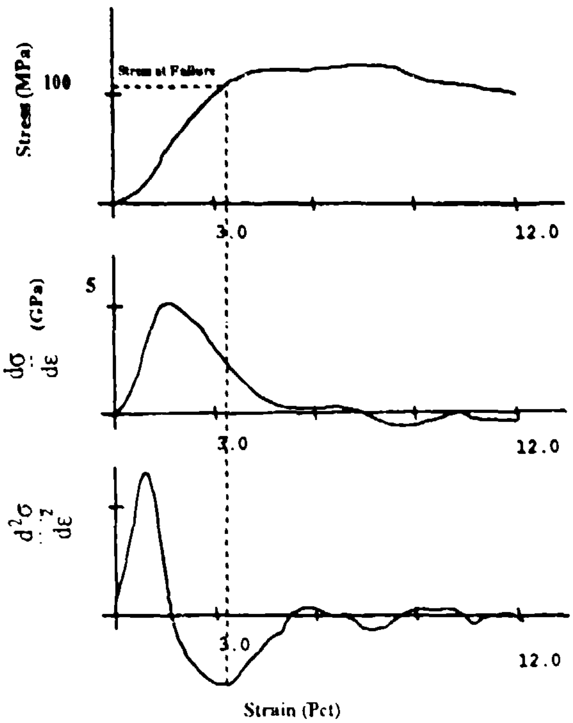

Figure 9. Illustration of the Method Used to Determine the Stress at Failure for M30 at 18°C

representing a combination of plastic and fracture failure. The value of the Stress at Failure was chosen at the point where the second derivative of the stress with respect to the strain is minimum. At this point yielding has already occurred, but it is not likely that much fracture generated surface area has been created. This is the point at which the greatest loss of strength is occurring, since the slope of the Stress vs Strain curve is decreasing most rapidly there. Other methods that may better characterize the mechanical response, which will be discussed later, are also under consideration. Using the information generated from these tests, Stress at Failure, Strain at Failure, and the Modulus can be plotted against temperature. This information is presented in Figures 10 through 12 for M30, JA2 and XM39, respectively.

All the curves in Figure 10 show a good linear fit. The correlation coefficient, R, for a least squares fit is 0.99, .98, and .97 for the Stress at Failure, Strain at Failure, and Modulus, respectively. Slightly better fits are obtained when the natural logarithm of these values is plotted against temperature. The resulting curves are found in Figure 13.

The curves for JA2, found in Figure 11, have a poor linear fit. When the natural logarithms of the Stress at Failure and Modulus values are plotted against temperature, shown in Figure 14, the linear fit is excellent (R = 1.00). The change in the nature of failure at -20°C is reflected the the Strain at Failure curves. At higher temperatures the material is getting stronger as the temperature is reduced, and below the transition temperature the material is becoming more brittle.

In contrast to the JA2, the XM39 curves found in Figure 12 have excellent linear fits. (R = 1.00 for both).The Strain at Failure curve indicates a strengthening at low temperatures. The large scatter, however, leaves this conclusion somewhat uncertain.

From these results constitutive equations can be generated to describe these quantities. These are given for the relationship that best fits the data in the following equations.

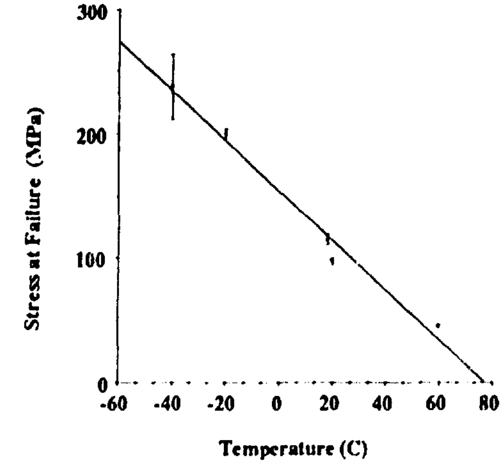

a. Stress at Failure vs Temperature

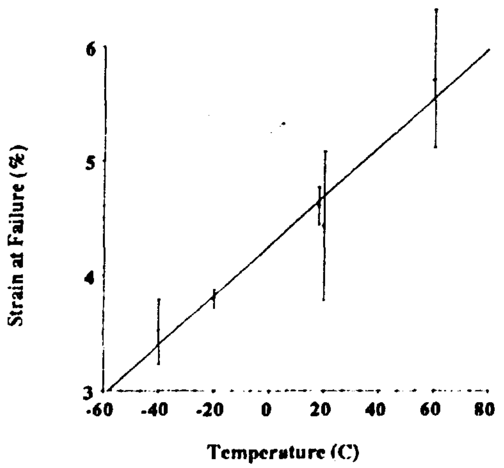

b. Strain at Failure vs Temperature

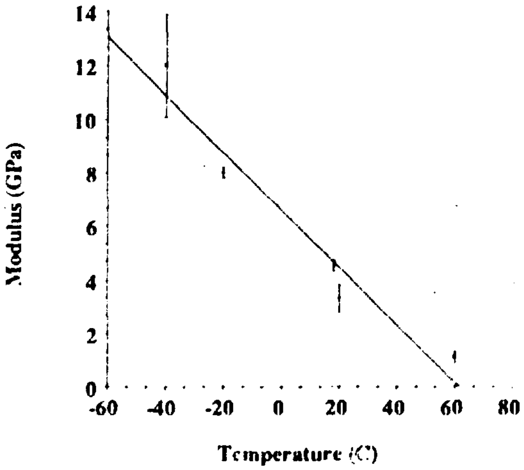

c. Modulus vs Temperature

Figure 10. Mechanical Response of M30 as a Function of Temperature

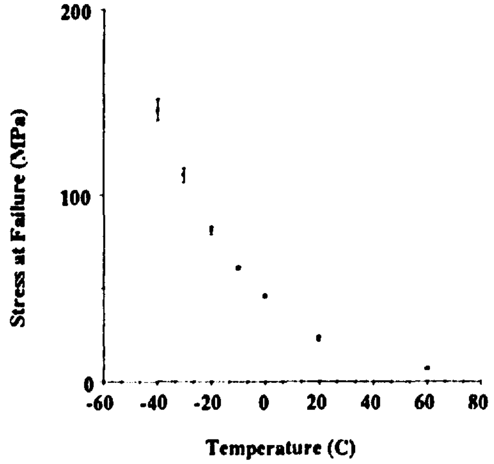

a. Stress at Failure vs Temperature

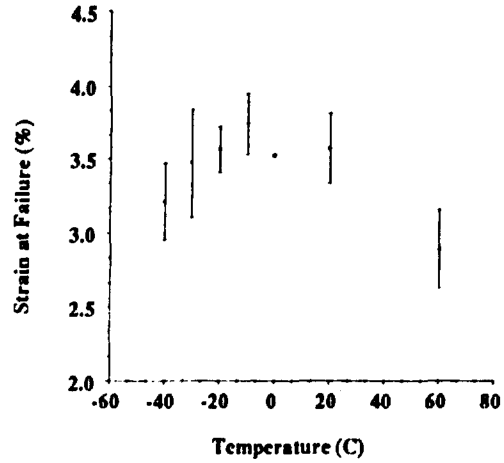

b. Strain at Failure vs Temperature

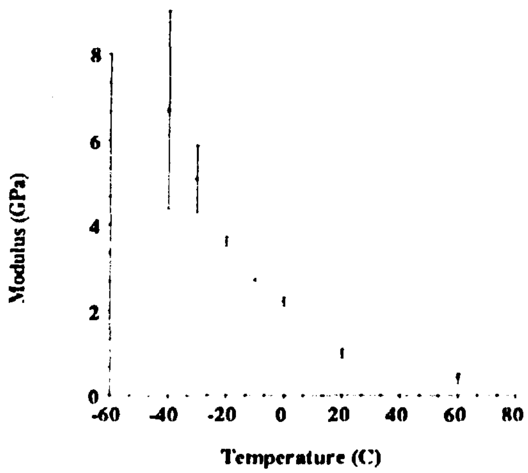

c. Modulus vs Temperature

Figure 11. Mechanical Response of JA2 as a Function of Temperature

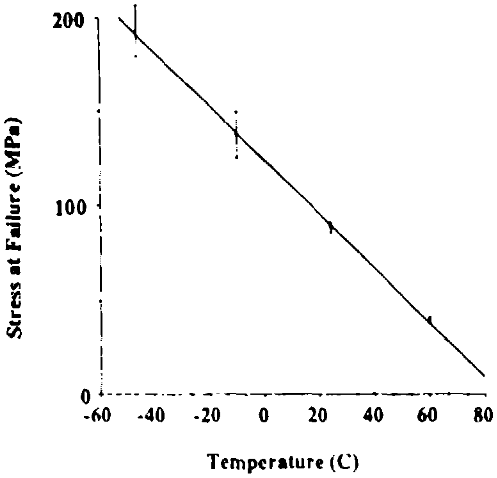

a. Stress at Failure vs Temperature

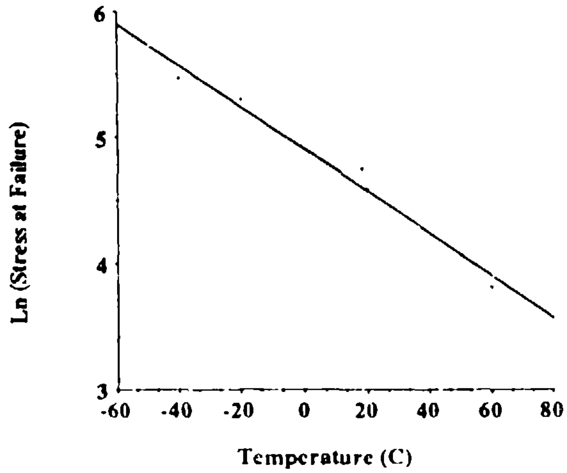

a. Ln [Stress at Failure] vs Temperature

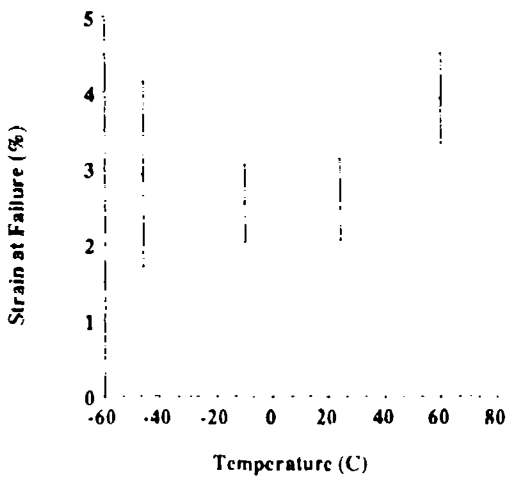

b. Strain at Failure vs Temperature

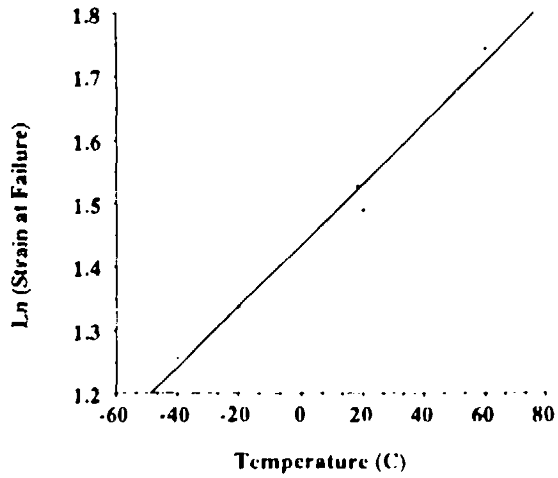

b. Ln [Strain at Failure] vs Temperature

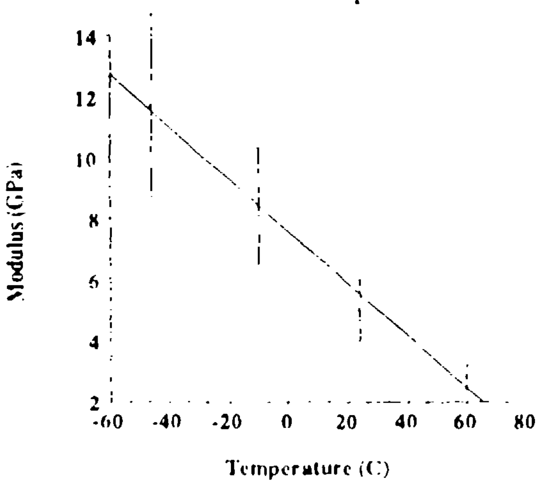

c. Modulus vs Temperature

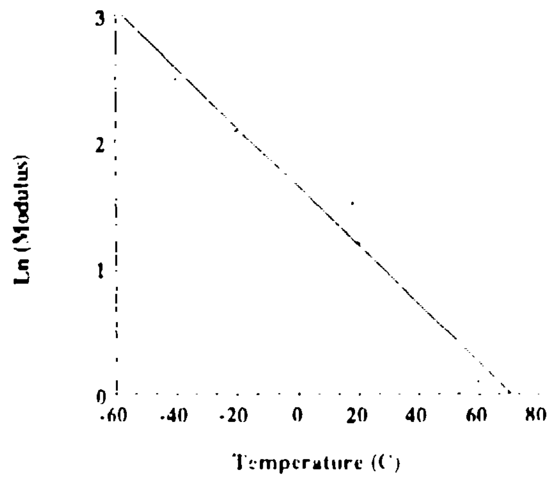

c. Ln [Modulus] vs Temperature

Figure 12. Mechanical Response of XM39 as a Function of Temperature

Figure 13. Natural Logarithm of the M30 Values Shown in Figure 11

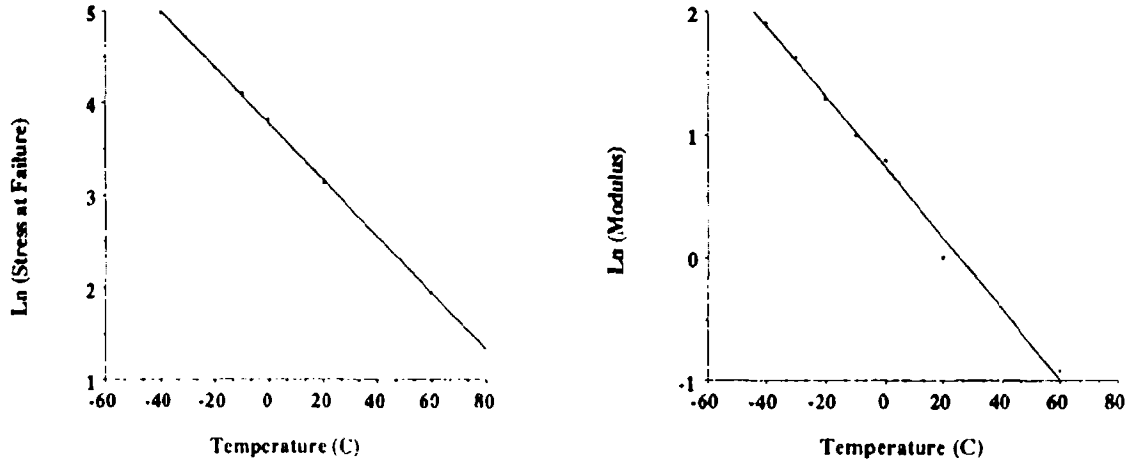

a. Ln [Stress at Failure] vs Temperature   b. Ln [Modulus] vs Temperature

Figure 14. Natural Logarithm of the JA2 Values Shown in Figure 12

For M30:

$$\sigma_f = 135\, e^{-0.0167\, T} \tag{2}$$

$$\varepsilon_f = 4.19\, e^{0.00481\, T} \tag{3}$$

$$E = 5.20\, e^{-0.0232\, T} \tag{4}$$

For JA2:

$$\sigma_f = 44.0\, e^{-0.0306\, T} \tag{5}$$

$$E = 2.07\, e^{-0.0287\, T} \tag{6}$$

For XM39:

$$\sigma_f = 125 - 1.45\, T \tag{7}$$

$$E = 7.57 - 0.0855\, T \tag{8}$$

where σ_f is in MPa, ε_f is in percent, E is in GPa, and T is in °C. Both JA2 and XM39 undergo transitions in this temperature range that result in the strain at failure experiencing an extreme.

B. High Pressure, High Rate Testing

Mechanical response testing was performed by Costantino and Ornellas[7,8] on JA2 and XM39 formulations to determine the character of the response at high pressures and high rates. In many cases the nature of the response changed. Instead of the brittle response that may have been experienced at ambient pressures, the response became more ductile in character and generally stronger as the pressures and rates were increased, although at higher rates the increase in ductility was not as noticeable as it was for higher pressures. Because of this change in response, it was not always meaningful or easy to assign a comparable failure stress that could be used for all pressures. In addition, the nature of the high pressure measurements required the shear stress, τ, to be determined. τ is defined as

$$\tau = (\sigma_1 - \sigma_3)/2 \qquad (9)$$

where σ_1 is the applied load, and σ_3 (equal to σ_2) is the ambient pressure. This definition causes a mismatch in the magnitudes of these measurements with respect to the ones obtained at BRL. However, by making some assumptions, the nature of the rate and pressure affects can be extracted from these measurements to provide constitutive relationships.

Figure 15a and 15b show the relationship of stress at three percent axial strain to the confining pressure at the various strain rates measured for JA2 and XM39. Figure 15c shows the Stiffness Modulus vs Confining Pressure for JA2. It can be seen that at higher pressures the stress and the modulus values increased linearly with pressure. Figure 16 shows the same variables plotted against the natural logarithm of the strain rate. If the Hopkinson split bar results (at atmospheric pressures) are deleted, the relationship also seems to be linear. These results are consistent with the behavior of other polymeric systems[9].

Constitutive equations can be extracted from these results. For JA2 the modulus and stress at 3 percent axial strain can be expressed in the following form:

$$E(P,\dot{\varepsilon}) = C_{E1}(P) + C_{E2}(P) \ln \dot{\varepsilon} \qquad (10)$$

$$\tau(P,\dot{\varepsilon}) = C_{\sigma1}(P) + C_{\sigma2}(P) \ln \dot{\varepsilon} \qquad (11)$$

where $C_{E1}(P)$, $C_{E2}(P)$, $C_{\sigma1}(P)$, and $C_{\sigma2}(P)$ are the pressure dependent linear coefficients derived from the curves plotted in Figure 16. These coefficients are plotted in Figures 17 and 18. The values for these coefficients are listed in Table 2. These equations can be made to reflect the temperature variation by making the assumption that temperature variations that occur at higher pressures and strain rates are similar to those that occur at atmospheric pressure. This assumption, while certainly not absolutely true, has merit, since curves of yield stress for polymeric materials taken at different temperatures and plotted for different strain rates fall into families of similar curves with similar slopes[7]. If this is done for JA2 the following equations result:

$$E(T,P,\dot{\varepsilon}) = [C_{E1}(P) + C_{E2}(P) \ln \dot{\varepsilon}]\, e^{-0.0287(T - T_0)} \qquad (12)$$

$$\tau(T,P,\dot{\varepsilon}) = [C_{\sigma1}(P) + C_{\sigma2}(P) \ln \dot{\varepsilon}]\, e^{-0.0306(T - T_0)} \qquad (13)$$

where T_0 determines the value of the variable at some reference temperature of interest and the other variables are as previously defined. Note that the logarithmic temperature dependence

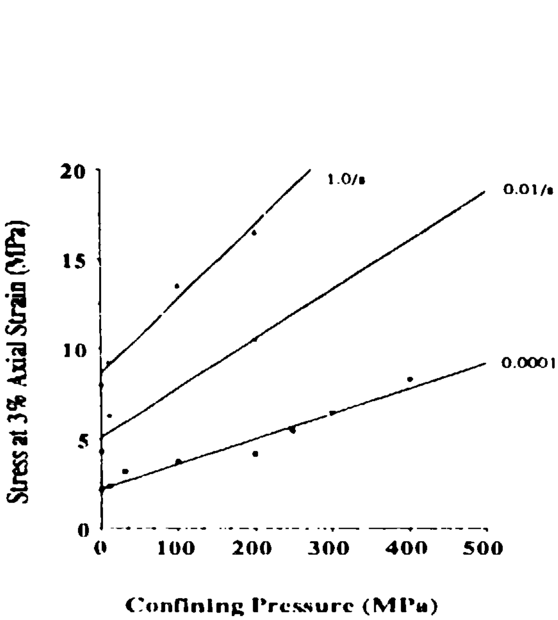

a. Stress at 3% Axial Strain vs Confining Pressure for JA2

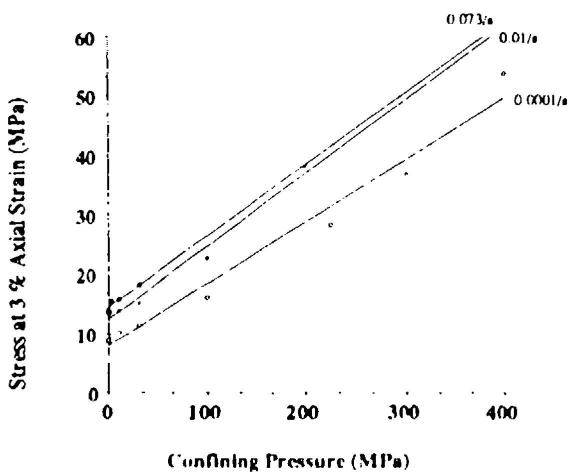

b. Stress at 3% Axial Strain vs Confining Pressure for XM39

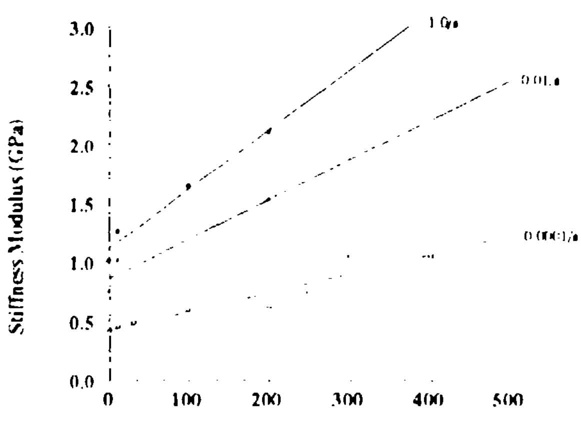

c. Modulus vs Confining Pressure for JA2

Figure 15. Mechanical Response of JA2 and XM39 as a Function of Confining Pressure

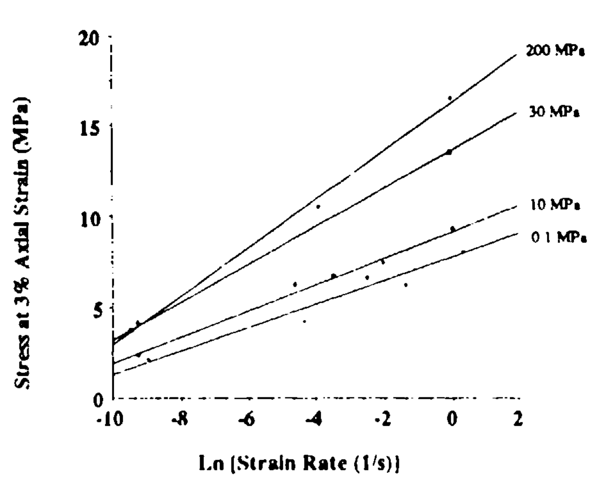

a. Stress at 3% Axial Strain vs Ln (Strain Rate) for JA2

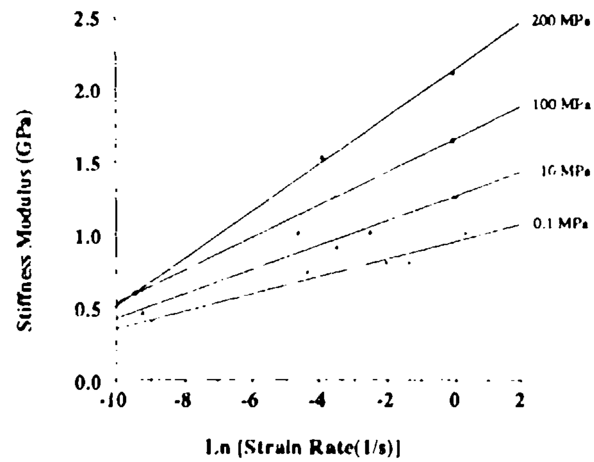

b. Stiffness Modulus vs Ln (Strain Rate) for JA2

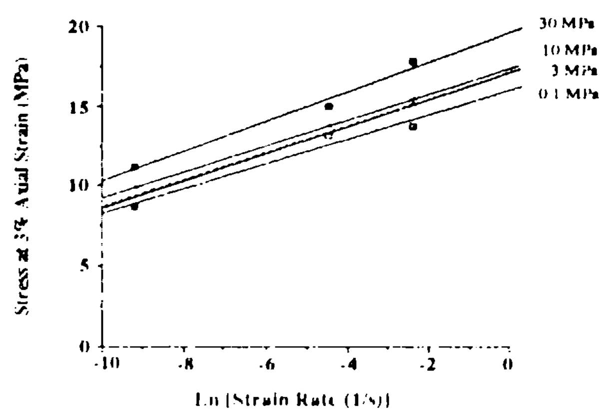

c. Stress at 3% Axial Strain vs Ln (Strain Rate) for XM39

Figure 16. Mechanical Response of JA2 and XM39 as a Function of Strain Rate

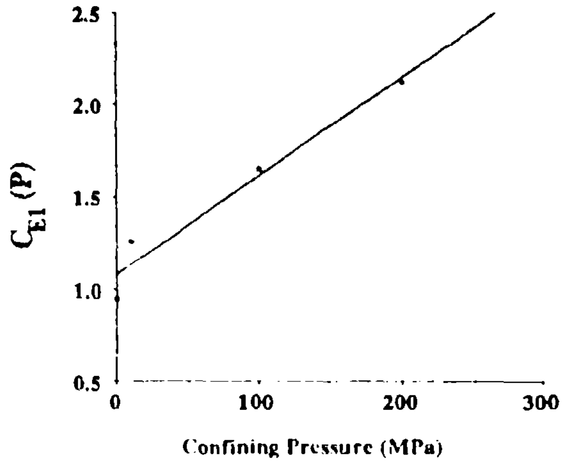

a. Constant Term Found in Equation 10

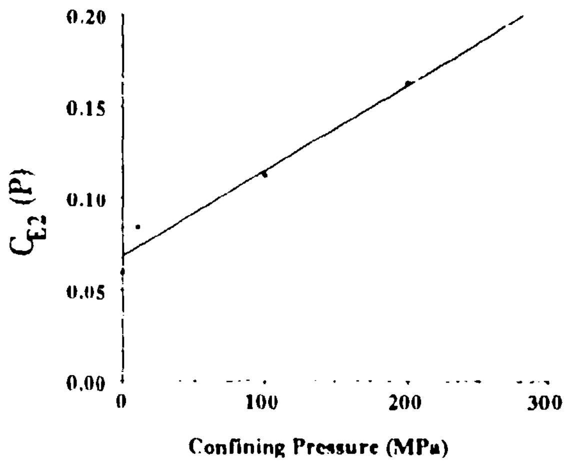

b. Constant Coefficient Found in Equation 10

Figure 17. Pressure Dependent Linear Constants Derived for the Modulus Values of JA2 from the Curves in Figure 16b

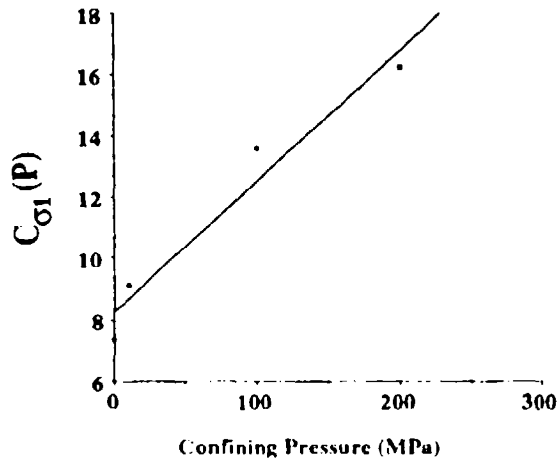

a. Constant Term Found in Equation 11

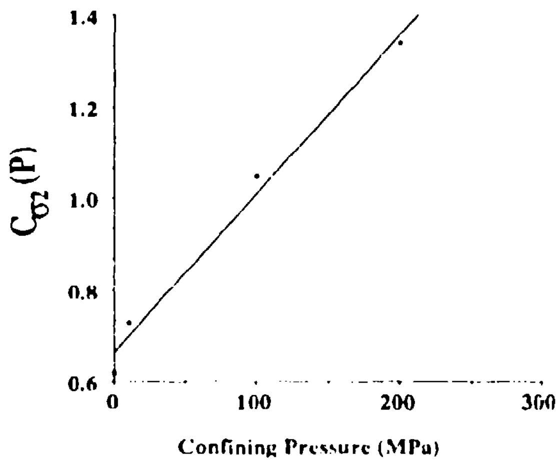

b. Constant Coefficient Found in Equation 11

Figure 18. Pressure Dependent Linear Constants Derived for the Stress Values of JA2 from the Curves in Figure 16a

permits the expression of the modulus and sheer stress at T_0 as a factor within the equation. Similar expressions can be derived for XM39 for the stress at three percent axial strain. The linear nature of the temperature dependence makes it more difficult to present a general expression for the stress. However, it can be seen from Figure 19 that the following expression can be derived in a fashion similar to those derived for JA2:

$$\tau(P,\varepsilon) = C_{\sigma 1}(P) + C_{\sigma 2}(P) \ln \dot{\varepsilon} \qquad (14)$$

where $C_{\sigma 1}(P)$ and $C_{\sigma 2}(P)$ are listed for XM39 in Table 2.

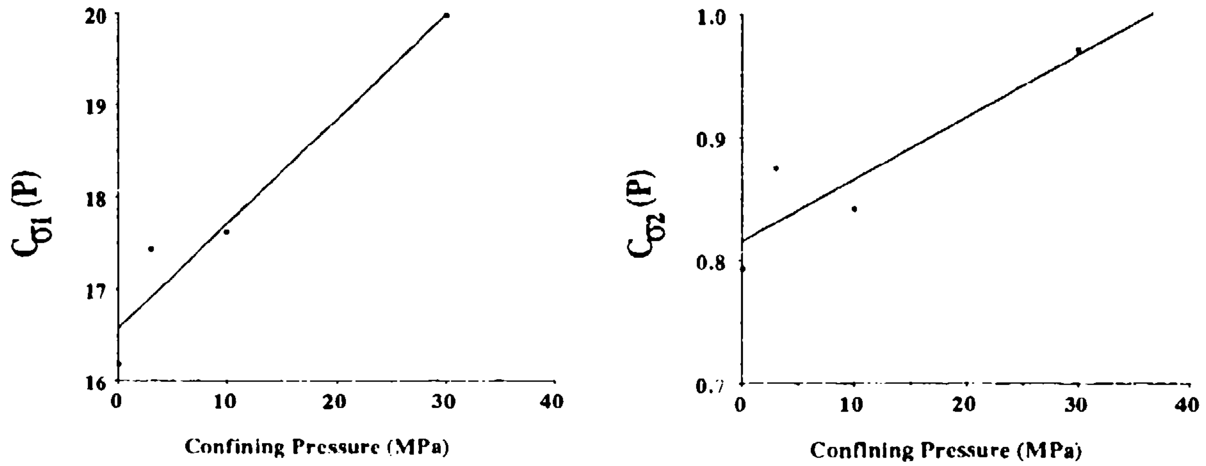

a. Constant Term Found in Equation 14   b. Constant Coefficient Found in Equation 14

Figure 19. Pressure Dependent Linear Constants Derived for the Stress Values of XM39 from the Curves in Figure 16c

Results for M30 are not yet available.

B. New Characterization Techniques

As expressed in other reports[10,11] new methods for characterizing the mechanical response of these materials are necessary. Conventional engineering measurements are still required, but they do not provide direct information as to how the mechanical response affects the interior ballistic conditions. A new method for post-failure characterization, the Normalized Failure Modulus, has been proposed[8] and correlates well with fracture generated surface area measurements that were gathered in other experiments. Mechanical response observations during the high pressure, high rate measurements performed at LLNL showed that conventional quantities, such as stress at failure and strain at failure, lose meaning due to dramatic changes in the

Table 2. Pressure Dependent Linear Constants for Equations 10 - 14

JA2	XM39
$C_{\sigma 1}(P) = 8.25\ \text{MPa} + 0.0427\ P$	$C_{\sigma 1}(P) = 16.6\ \text{MPa} + 0.114\ P$
$C_{\sigma 2}(P) = 0.663\text{MPa} + 0.00347\ P$	$C_{\sigma 2}(P) = 0.815\text{MPa} + 0.00503\ P$
$C_{L1}(P) = 1.08\ \text{GPa} + 0.00536\ \text{GPa/MPa}\ P$	
$C_{L2}(P) = 0.0681\ \text{GPa} + 0.000470\ \text{GPa/MPa}\ P$	

Note: P, the confining pressure, has units of MPa strength and mode of failure found for propellants under these conditions. It is thought that measurements that characterize the whole response curve are required for proper evaluation. The method of evaluation that is developed will require the results of an extensive testing program, which is currently under way.

IV. CONCLUSIONS AND FUTURE EFFORTS

Mechanical properties measurements have been performed on M30, JA2, and XM39 gun propellants at various strain rates, temperatures, and pressures. The procedure used to obtain these high rate results is documented in this report. Results from numerous tests resulted in constitutive equations that describe the mechanical response as a function of temperature, pressure, and strain rate. These equations may be used in interior ballistic codes to express the mechanical state of the material under interior ballistic conditions.

Many new and expanded test programs are planned for these propellants. High pressure measurements, similar to those performed on JA2 and XM39 propellants, are planned for M30 at LLNL. Upon completion of these tests similar constitutive equations will be generated. Tests will be performed to characterize the post-failure response of these propellants, as indicated above. Other testing will characterize the stress and strain relaxation of these materials over the temperature range of ballistic interest. Finally, propellant bed mechanical response and fracture generated surface area evaluation will be characterized and correlated with single grain response.

V. ACKNOWLEDGMENTS

The author would like to especially thank Mike Leadore who gathered a significant portion of these data with great care and diligence. Also, thanks are due to Tom Fischer, who helped program the data acquisition and reduction software.

REFERENCES

1. F. W. Robbins, A. W. Horst, "A Simple Theoretical Analysis and Experimental Investigation of Burning Processes for Stick Propellant," Memorandum Report (ARBRL-MR-03295), USA Ballistic Research Laboratory, Aberdeen Proving Ground, Maryland, July 1983.

2. F. W. Robbins, A. W. Horst, "Continued Study of Stick Propellant Combustion Processes," Memorandum Report (ARBRL-MR-03296), USA Ballistic Research Laboratory, Aberdeen Proving Ground, Maryland, July 1983.

3. R. J. Lieb, J. J. Rocchio, and A. A. Koszoru, "Impact Mechanical Properties Tester for Gun Propellants," Proceedings of 1981 JANNAF Structures and Mechanical Behavior Subcommittee Meeting, Vol.1, CPIA Publication 351, pp 155-173, December 1981.

4. R. J. Lieb, "Surface Area Analysis of Grain-Grain Impact of Gun Propellants,"1986 JANNAF Structures & Mechanical Behavior Subcommittee Meeting, CPIA Publication 449, pp 109-116, April 1986.

5. R. J. Lieb, "Uniaxial Compressive Gun Propellant Test," Tentative Standard for CPIA Publication 21 Solid Propellant Mechanical Properties Manual. 1988

6. R. J. Lieb, D. Devynck, and J. J. Rocchio, "The Evaluation of High Rate Fracture Damage of Gun Propellant Grains," 1983 JANNAF Structure and Mechanical Behavior Subcommittee Meeting, CPIA Publication 388, pp 177-185, November 1983.

7. M. Costantino and D. Ornellas, "Initial Results for the Failure Strength of a LOVA Gun Propellant at High Pressures and Various Strain Rates," 1985 Propulsion Meeting, CPIA Publication 425, Volume I, pp 213-227, April 1985.

8. M. Costantino and D. Ornellas, " High Pressure Failure Curve for JA2," 1987 JANNAF Structures & Mechanical Behavior Subcommittee Meeting, CPIA Publication 463, Volume I, pp 73-80, March 1987.

9. I. M. Ward, "Mechanical Properties of Solid Polymers," Second Edition, John Wiley & Sons, New York, 1983, pp357-384.

10. R. J. Lieb, "Impact-Generated Surface Area in Gun Propellants," Technical Report (BRL-TR-2946, AD A200468), USA Ballistic Research Laboratory, Aberdeen Proving Ground, Maryland, November 1988.

11. R. J. Lieb, "High Rate Intrinsic Bed Response of Gun Propellant," 1987 JANNAF Structures & Mechanical Behavior Subcommittee Meeting, CPIA Publication 463, Volume I, pp 51-62, March 1987.

APPENDIX A

DATA ACQUISITION AND REDUCTION

APPENDIX A

Drop Weight Data Acquisition & Reduction Program Outline

Name: DWDAR
Location: Program Disk, Track 01
Function: Drop Weight Data Acquisition and Reduction.

Registers: I - Integer that keeps track of data stroage and retrieval. Initially, if data disk is in drive 1, I = 1YY, where YY = part of the Sample ID.

Sample Information:
A - (L) Sample Length (mm).
B - (D) Sample Diameter (mm).
C - (PD) Perforation Diameter (mm).
D - (PN) Perforation Number.
E - (XA) Net Cross Sectional Area (mm^2), Calculated.

Test Information:
A' - Optical Displacement Follower Calibration (mm/V).
B' - Force Transtucer Calibration (N/V).
C' - (T) Temperature (℃).
D' - (DH) Drop Height (cm).
E' - (DW) Drop Weight (kg).
R9 - (ID) Sample ID (Norland DW Data Disk #, XX, plus First Track #, YY, i.e. if XX = 36 and YY = 17 the Sample ID = 36.17).

Calculated Engineering Parameters:
R1 - (MS) Maximum Stress (MPa).
R2 - (FS) Stress at Failure, Yield Stress (MPa).
R3 - (SF) Strain at Failure, Yield Strain (%).
R4 - (SR) Strain Rate (sec^{-1}).
R5 - (E) Elastic Modulus, Uniaxial Compressional (GPa).
R6 - (ED) Actual Absorbed Energy Density (MJ/m^3 or MPa).
R7 - (TD) Maximum Thoretical Absorbed Energy Density (MPa).

Instructions:

1. Set registers A, B, C, D, A', B', C', D', E', R9, and I to the proper values.

2. Acquire data such that a base line of at least 100 points exists with displacement in H1, and force in H2 (usually 7/8's trigger presave setting does this).

3. Run.

4. Follow prompts so that:
   a. At first pause set P to maximum stress.
   b. At next pause set P to stress at failure.
   c. At next pause set P and Q so slope measures strain rate for compression before failure.
   d. At next pause set P and Q so slope measures modulus for compression before failure.

5. Registers (above) are printed and stress and strain plots may be printed, along with stress vs strain before failure. Prompts guide selection. Sample and test information are made ready for the next drop. Changes are required if different drop height, sample size, etc. are used.

DWDAR Program

The following program was used to acquire and analyse the data from the Drop Weight Mechanical Properties Tests. The program was used on a Norland Processing Digital Oscilliscope, Model 3001A, with dual disk storage capability.

Program	Comment
0001 TRG.H	Set Trigger
0002 0 ==> R0	Initialize Registers
0003 0 ==> R1	
0004 0 ==> R2	
0005 0 ==> R3	
0006 0 ==> R4	
0007 0 ==> R5	
0008 0 ==> R6	
0009 0 ==> R7	
0010 0 ==> E	
0011 DPLY Q1 ==> DISK 1 DISK	Store Raw Data
0012 INCI	
0013 DPLY Q2 ==> DISK 1 DISK	
0014 INCI	
0015 DPLY Q3 ==> DISK 1 DISK	
0016 INCI	
0017 DPLY Q4 ==> DISK 1 DISK	
0018 ERAS ERAS	Display I and Specimen ID
0019 DPLY I DPLY	
0020 DPLY "ID = DPLY R9 "	
0021 H2 * 1 +/- ==> H2	Invert Force Curve

Program	Function
0022 0 ==> HSETP 0023 100 ==> HSETQ 0024 HSETP 0025 HSETQ	Set P & Q Cursors on Displacement Baseline
0026 STAT H1 VS T/F 0027 H1 - C' ==> H1	Zero Displacement
0028 15 NPAVG H1	Smooth Displacement
0029 PNEXT 0030 PNEXT 0031 QNEXT 0032 QNEXT	Set P & Q Cursors on Force Baseline
0033 STAT H2 VS T/F 0034 H2 - C' ==> H2	Zero Force
0035 I - 3 ==> I 0036 DISK I ==> A'	Restore Primed Registers
0037 A' / A ==> R0 0038 R0 * 100 ==> R0 0039 R0 * H1 ==> H1	Convert Displacement to Strain (%)
0040 B * B ==> R0 0041 R0 * .7854 ==> R0 0042 C * C ==> R1 0043 R1 * .7854 ==> R1 0044 R1 * D ==> R1 0045 R0 - R1 ==> R0 0046 R0 ==> E	Calculate Net Area
0047 B' / R0 ==> R0 0048 R0 * H2 ==> H2	Convert Force to Stress (MPa)

```
0049 C' - 20 ==> R0
0050 R0 * 5.4 EXP 04 +/- ==> R0
0051 1 + R0 ==> R0
0052 H2 / R0 ==> H2
```

Temperature Correction for Force Gage

```
0053 I + 4 ==> I
0054 DPLY Q1 ==> DISK I DISK
0055 INCI
0056 DPLY Q2 ==> DISK I DISK
0057 INCI
0058 DPLY Q3 ==> DISK I DISK
0059 INCI
0060 DPLY Q4 ==> DISK I DISK
```

Store Stress and Strain

```
0061 I - 7 ==> I
0062 DISK I "RAW DISP 1/2"
0063 INCI
0064 DISK I "RAW DISP 2/2"
0065 INCI
0066 DISK I "RAW F 1/2"
0067 INCI
0068 DISK I "RAW F 2/2"
0069 INCI
0070 DISK I "STRAIN 1/2"
0071 INCI
0072 DISK I "STRAIN 2/2"
0073 INCI
0074 DISK I "STRESS 1/2"
0075 INCI
0076 DISK I "STRESS 2/2"
```

Label Data Tracks

```
0077 DPLY "PLACE P AT MAX STRESS"
0078 PAUSE
0079 PAUSE
0080 ERAS ERAS
0081 COOR
```

Record and Store Maximum Stress (MS)

```
0082 V ==> R1
0083 DPLY "PLACE P AT FAILURE STRESS"
0084 PAUSE
0085 PAUSE
0086 ERAS ERAS
0087 COOR
```

Record and Store Failure Stress (FS)

```
0088 V ==> R2
0089 PNEXT
0090 PNEXT
0091 COOR
```

Record and Store Strain at Failure (SF)

```
0092 V ==> R3
0093 QNEXT
0094 QNEXT
0095 H1 / 100 ==> H1
0096 DPLY "PLACE  P AND Q TO MEASURE
     STRAIN RATE"
0097 PAUSE
0098 PAUSE
0099 ERAS  ERAS
0100 STAT H1 VS T/F
0101 H' ==> R4
```

Record and Store Strain Rate (SR)

```
0102 0 ==> DRAW A
0103 R3 / 100 ==> R0
0104 R0 ==> DRAW B
0105 DRAW  H2 VS H1
0106 DPLY "PICK  BEST LINE  FOR E -  THEN RUN"
0107 PAUSE
0108 PAUSE
0109 ERAS  ERAS
0110 PNEXT
0111 PNEXT
0112 QNEXT
0113 QNEXT
0114 DPLY H2  VS H1
0115 DPLY "PLACE  P AND Q  TO BEST LINE"
0116 PAUSE
0117 PAUSE
0118 ERAS ERAS
0119 DPLY H1  H2 VS T/F
```

Record and Store Modulus (E)

```
0120 STAT H2  VS H1
0121 H' / 1000 ==> R5
0122 390 * A ==> R0
0123 R0 / E ==> R0
0124 1 - R0 ==> R0
0125 1 / R5 ==> R5
0126 R5 - R0 ==> R5
```

Correct Modulus for Rig Compliance

```
0127  1/R5 ==> R5
0128  D/DX H1 ==> H1
0129  H1 * H2 ==> H1
0130  HSETP
0131  2048 ==> HSETQ
0132  HSETQ
```

Calculate and Store Energy Density (ED)

```
0133  INTPQ ==>  R6
0134  I - 7 ==> I
0135  DISK I ==> A'
0136  D'* E' ==> R0
0137  R0 * 98.1 ==> R0
0138  A * E ==> R7
```

Calculate and Store Maximum Theoretical Energy Density (TD)

```
0139  R0 / R7 ==> R7
0140  I + 4 ==> I
0141  D DISK I DISK
0142  DISK I ==> Q1
0143  DPLY Q1 ==> DISK I DISK
```

Store Calculated Engineering Parameters and Label

```
0144  DISK I "STRAIN (1/2)"
0145  INCI
0146  DISK I ==> Q2
0147  2 + I ==> I
```

Display Stress and Strain

```
0148  DPLY H1 H2 VS T/F
0149  PRINT R9 A' B' C' D' E' PRINT
0150  PRINT A B C D E PRINT
0151  PRINT R1 R2 R3 R4 R5 R6 R7 PRINT
```

Report Data

```
0152 DPLY "SELECT PLOT REGION WITH P-Q
     ON H1"
0153 DPLY "OR  GOTO 200 AND RUN"
0154 PAUSE
0155 PAUSE
```

Option for Further Analysis

```
0156 LABL H1 "   STRAIN  (PCT)"
0157 LABL T/F H1 "       TIME (S)"
0158 LABL T/F H2 "       TIME (S)"
0159 LABL  H2 "   STRESS (MPA)"
```

Label Plot Axes

```
0160 ERAS ERAS
0161 DRAW  UPPR H1 VS T/F
0162 PNEXT
0163 PNEXT
0164 QNEXT
0165 QNEXT
0166 DRAW LOWR  H2 VS T/F
0167 DPLY  DPLY
0168 ERAS ERAS
0169 DPLY "DROP  WEIGHT"
0170 DPLY "IMPACT  TEST"
0171 DPLY " "
0172 DPLY " "
0173 DPLY "ID = DPLY R9 "
0174 DPLY " "
0175 DPLY " "
0176 DPLY "L  = DPLY A MM"
0177 DPLY "D  = DPLY B MM"
0178 DPLY "PD = DPLY C MM"
```

Build Report Display

```
0179 DPLY "PN = DPLY D"
0180 DPLY "XA = DPLY E SMM"
0181 DPLY " "
0182 DPLY " "
0183 DPLY "T = DPLY C' C"
0184 DPLY "DH = DPLY D' CM"
0185 DPLY "DW = DPLY E' KG"
0186 DPLY " "
0187 DPLY " "
0188 DPLY "MS = DPLY R1 MPA"
0189 DPLY "FS = DPLY R2 MPA"
0190 DPLY "SF = DPLY R3 PCT"
0191 DPLY "SR = DPLY R4 1/S"
0192 DPLY "E = DPLY R5 GPA"
0193 DPLY "ED = DPLY R6 MPA"
0194 DPLY "TD = DPLY R7 MPA"
```

Build Report Display

```
0195 PAUSE
0196 PAUSE
```

Print Display Option

```
0197 R3 ==> DRAW B
0198 DRAW H2 VS H1
```

Stress vs Strain Report Display

```
0199 PAUSE
0200 PAUSE
```

Print Display Option

```
0201 .08 + R9 ==> R9
0202 INCI
0203 ERAS ERAS
0204 DPLY H1 H2 VS T/F
0205 DPLY A B I R9 DPLY
0206 END
```

Increment I and Data ID for Next Acquisition

APPENDIX B

UNIAXIAL COMPRESSIVE GUN PROPELLANT TEST

APPENDIX B

UNIAXIAL COMPRESSIVE GUN PROPELLANT TEST

1 Scope.

This method covers the determination of the mechanical properties of composite propellants loaded in compression at high strain or loading rates. Test specimens of standard shape are recommended, but due to the nature of propellant formulation and production, non-standard specimen testing is also included.

These tests provide information on the compressive mechanical properties of composite propellant grains at high strain rates. Since gun performance and safety are influenced by the mechanical response of the grains under interior ballistic conditions, measurements made under similar conditions are of great importance.

The compressive properties include the yield stress (stress at failure), the yield strain (strain at failure), and the modulus of elasticity. Normally the yield stress will be measured at the yield point, but at low temperatures where brittle fracture occurs before yield, the maximum stress at fracture will be the yield stress. The compressive strength has a well defined value only for materials that are relatively brittle, a property that is specifically avoided in propellant design. Compressive strength is, therefore, not measured.

These tests provide information on the mechanical response of propellant samples as a function of temperature, strain rate, and energy density. This information can be used to establish desirable propellant mechanical properties, to determine mechanical response transitions, and for quality control. Not enough information is available yet for these tests to be used for design applications.

The standard units for measurement are SI units.

2 Definitions.

2.1 Compressive Stress (nominal). The compressive load per unit net area of the original cross section carried by the specimen at any time. Stress is expressed in force per unit area.

2.2 Compressive Deformation. The decrease in specimen length along the longitudinal axis produced by the compressive load. It is expressed as units of length.

2.3 Compressive Strain. The ratio of the compressive deformation to the specimen length, i.e., the change in specimen length per original specimen length along the longitudinal axis. Strain has dimensions of unity.

2.4 Percentage Compressive Strain. The compressive deformation of a specimen expressed as a percentage of the original specimen length.

2.5 Compressive Stress-Strain Diagram. A diagram which has the compressive values of stress on the ordinate axis plotted against the corresponding strain values on the abscissa. The locus of points is called the compressive stress-strain curve.

2.6 Compressive Yield Point. The point on the compressive stress-strain curve at which plastic failure is evidenced by a deviation from the linear stress-strain relationship.

2.7 Compressive Yield Stress (nominal). The compressive stress at the yield point.

2.8 Compressive Stress at Failure (nominal). The compressive stress at the yield point for plastic failure, and at fracture for brittle failure.

2.9 Strain Rate. The slope in the linear region of the compressive strain plotted against time before failure. The strain rate is measured in inverse time.

2.10 Compressive Modulus of Elasticity. The slope of the best straight line in the linear region of the compressive stress-strain curve for which the strain rate is constant. The modulus has units of force per unit area.

2.11 Impact Energy Density. The integral of the compressive stress with respect to the compressional strain over the entire impact. The energy density has units of energy per unit volume or pressure.

3 Test Apparatus.

3.1 Testing Machine. Any compressive testing machine may be used that is able to record simultaneous force and displacement information at crosshead speeds that result in strain rates up to the order of 100 sec^{-1}. This may include high rate servo-hydraulic or drop weight impact testers.

3.2 Displacement (Deformation) Measurement. The specimen deformation should by measured directly by a system with a response time small enough to ensure simultaneous displacement-load recordings. The machine compliance should be determined and if it is found to be significant, corrections to the deformation should be made. Measurements should indicate displacement within ± 1 percent of maximum.

3.3 Load Measurement. The load measurement must reflect the total compressive load carried by the specimen. The mechanism must have a response time fast enough to ensure simultaneous displacement-load recordings, and must have a low inertial mass. Measurements should indicate load within ± 1 percent of maximum.

3.4 Compression Tool. The compression tool must apply the compressive load to the specimen so that noncoaxial specimen loads due to the device are insignificant before failure.

3.5 Calibration. Each component of the testing device should be calibrated according to the manufacturer's recommended schedule. The entire system should be standardized with a known material under conditions as close as possible test conditions. If this is not possible, then steps should be taken to ensure that measurements are as accurate and consistent as possible.

4 Test Specimens.

The test specimens will be right cylinders with a uniform circular cross section. The specimens shall be selected for testing in a random manner. Any nonrandom qualification, such as reoccurring specimen defect, that prevents selection of specimens contained within the population must be noted. The length to diameter ratio shall be one, and the interior of the specimen shall either be uniform solid or contain symmetric perforations (single, or multiple) parallel to the cylinder axis. The specimen ends will be flat and parallel to 0.025 mm and perpendicular to the longitudinal axis to within 0.5°. Any deviation from this description must be noted in the presentation of results.

The specimen ends shall be prepared so no fracture damage is induced. All particles that result from the end preparation shall be carefully removed from the specimen before testing in a manner that does not result in grain damage.

Perforation diameter shall be measured on each perforation of a specimen after end preparation by pin gages. Measurements should be taken on enough specimens to ensure that a representative measurement is made. Specimens on which perforation measurements are made should not be used for testing.

Specimen storage shall be at 20 ± 5°C in sealed containers until testing or conditioning procedures begin.

Testing shall be done with no lubricant added to the end surfaces. If any contamination or additive is present during testing, a statement on the surface conditions must be included in the report.

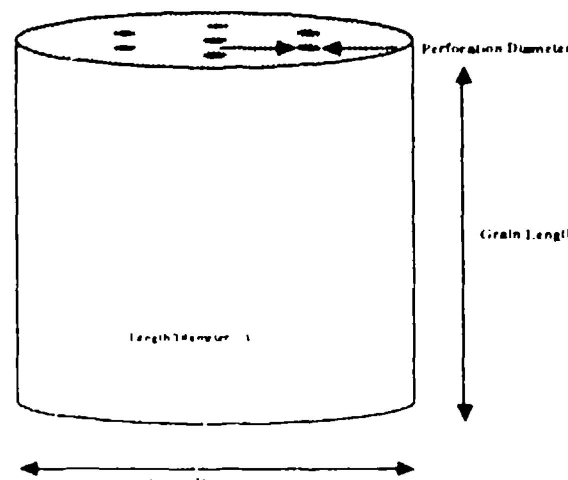

Typical 7-Perforated Specimen

5 Test Method.

5.1 Measurement of Test Specimen Dimensions. Each dimension shall be measured at least three times using an instrument or technique that permits accuracy and precision to within 1% of the measured dimension. Each specimen length and diameter shall be measured prior to conditioning or testing. The perforation diameter of the specimens shall have been determined as outlined above, and may be assumed to be accurate for the test specimen.

5.2 Specimen Conditioning. For those tests where temperature conditioning is required, each specimen shall be conditioned within one Celsius degree of the planned test temperature for at least one hour before testing. Room temperature is 23 ± 2°C.

For samples requiring conditioning, the conditioned specimen shall be placed into a temperature controlled region of the test apparatus. After the specimen has been transferred, the test temperature shall be maintained within the testing region for a period long enough to ensure that any disruption of the conditioning of the specimen has been corrected.

If specimens are tested at other than ambient pressures, the pressure history of the specimen must be recorded for each tested sample.

5.3 Test Procedure. Care will be taken to assure uniform straining. Any procedure that permits non-axisymmetric loading will not be utilized. The actuator (or ram) velocity will be as uniform as possible. At least five specimens shall be tested under each testing condition. If large deviations from average values result, additional tests should be performed in order to determine the nature of the scatter.

Simultaneous force and displacement data, stress and strain calculations, specimen dimensions, test conditions, gage calibrations, and a photograph of a typical damaged grain should be recorded and kept as a permanent data file. The complete propellant lot number, as found on the propellant description sheet, should be kept as the primary identifier of the propellant specimen tested. Any test identification system should be directly linked to the lot number.

Samples should be taken to failure at the desired strain rate.

6 Data Reduction.

6.1 Calculations. Stress shall be determined by Definition .2.1, where net area is the total cross sectional area less any perforation or other area not supporting the applied load. Strain values are determined by Definition 2.3. Compliance corrections to displacement shall be included in any calculations except when reporting "raw" data. All other calculations will be in accordance with the definitions listed in 2 or be explained in the report containing the test results.

6.2 Report. The report of test results shall include at least the following: Complete identification of the sample, including the source, formulation, identification numbers, and history; a statement of how the specimens were prepared, and the testing conditions used; a reference to, or description of the impact tester used; the total number of specimens tested per test condition; the compressive stress at failure in MPa, compressive strain at failure in percent, compressive modulus of elasticity, in GPa, strain rate in sec^{-1}, and standard deviation for each of these measurements; a failure characterization, a representative compressive stress-strain diagram, and a representative photograph of a tested specimen.

ASTM References

D 256 Impact Resistance of Plastics and Electrical Insulating Materials
D 621 Deformation of Plastics Under Load
D 638 Test for Tensile Properties of Plastics
D 695 Compressive Properties of Rigid Plastics
D 732 Shear Strength of Plastics by Punch Tool
D 746 Brittleness Temperature of Plastics and Elastomers by Impact
D 1621 Compressive Properties of Rigid Cellular Plastics

APPENDIX C

ILLUSTRATION OF MEASURED PARAMETERS

APPENDIX C

Illustration of Measured Parameters

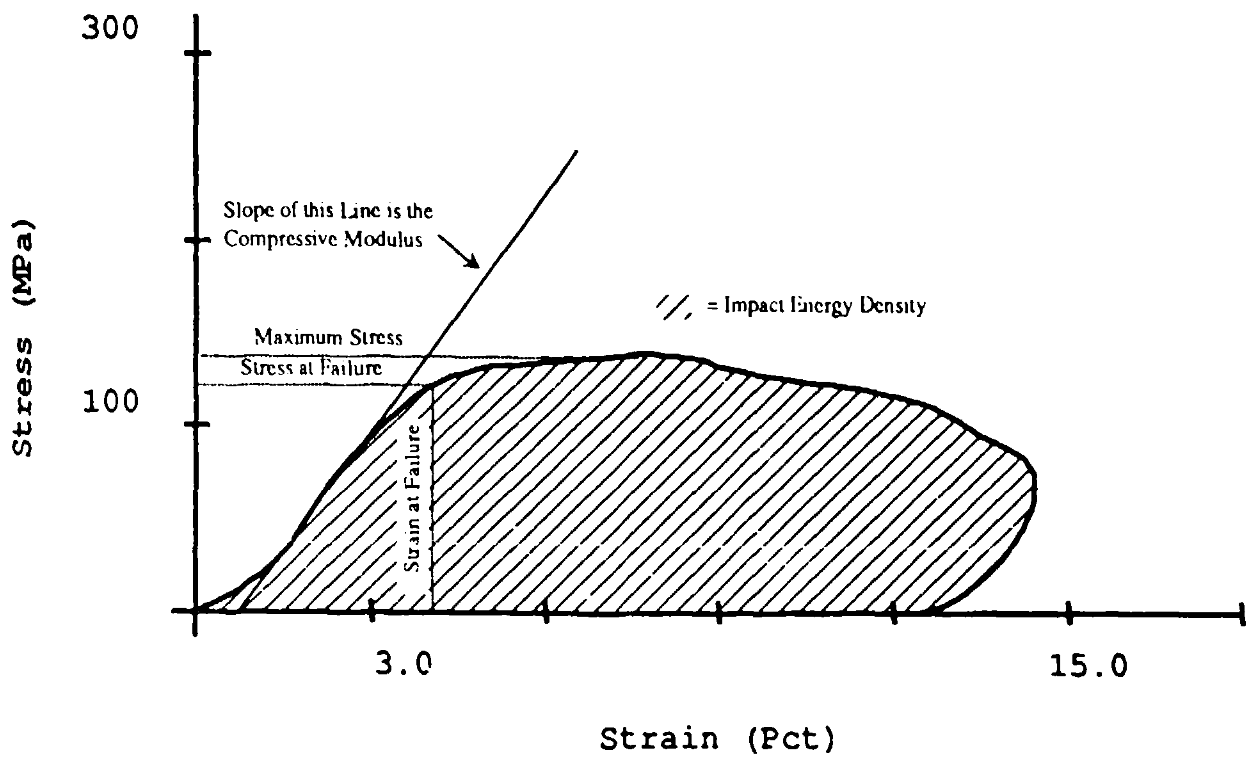

BRL MANDATORY DISTRIBUTION LIST

No of Copies	Organization
(Unclass., unlimited) 12 (Unclass., limited) 2 (Classified) 2	Administrator Defense Technical Info Center ATTN: DTIC-DDA Cameron Station Alexandria, VA 22304-6145
1	HQDA (SARD-TR) Washington, DC 20310-0001
1	Commander US Army Materiel Command ATTN: AMCDRA-ST 5001 Eisenhower Avenue Alexandria, VA 22333-0001
1	Commander US Army Laboratory Command ATTN: AMSLC-DL Adelphi, MD 20783-1145
2	Commander Armament RD&E Center US Army AMCCOM ATTN: SMCAR-MSI Picatinny Arsenal, NJ 07806-5000
2	Commander Armament RD&E Center US Army AMCCOM ATTN: SMCAR-TDC Picatinny Arsenal, NJ 07806-5000
1	Director Benet Weapons Laboratory Armament RD&E Center US Army AMCCOM ATTN: SMCAR-LCB-TL Watervliet, NY 12189-4050
1	Commander US Army Armament, Munitions and Chemical Command ATTN: SMCAR-ESP-L Rock Island, IL 61299-5000
1	Commander US Army Aviation Systems Command ATTN: AMSAV-DACL 4300 Goodfellow Blvd. St. Louis, MO 63120-1798
1	Director US Army Aviation Research and Technology Activity Ames Research Center Moffett Field, CA 94035-1099

No of Copies	Organization
1	Commander US Army Missile Command ATTN: AMSMI-RD-CS-R (DOC) Redstone Arsenal, AL 35898-5010
1	Commander US Army Tank Automotive Command ATTN: AMSTA-TSL (Technical Library) Warren, MI 48397-5000
1	Director US Army TRADOC Analysis Command ATTN: ATAA-SL White Sands Missile Range, NM 88002-5502
(Class. only) 1	Commandant US Army Infantry School ATTN: ATSH-CD (Security Mgr.) Fort Benning, GA 31905-5660
(Unclass. only) 1	Commandant US Army Infantry School ATTN: ATSH-CD-CSO-OR Fort Benning, GA 31905-5660
(Class. only) 1	The Rand Corporation P.O. Box 2138 Santa Monica, CA 90401-2138
1	Air Force Armament Laboratory ATTN: AFATL/DLODL Eglin AFB, FL 32542-5000

Aberdeen Proving Ground

Dir, USAMSAA
ATTN: AMXSY-D
AMXSY-MP, H. Cohen

Cdr, USATECOM
ATTN: AMSTE-TO-F

Cdr, CRDEC, AMCCOM
ATTN: SMCCR-RSP-A
SMCCR-MU
SMCCR-MSI

DISTRIBUTION LIST

No. Of Copies	Organization
1	Commander US Army War College ATTN: Library-FF229 Carlisle Barracks, PA 17013
1	Project Manager Cannon Artillery Weapons System, ARDEC, AMCCOM ATTN: AMCPM-CWW F. Menke Dover, NJ 07801-5001
1	Cannon Artillery Weapons System, ARDEC, AMCCOM ATTN: AMCPM-CWS M. Fisette Dover, NJ 07801-5001
1	Cannon Artillery Weapons System, ARDEC, AMCCOM ATTN: AMCPM-CWA H. Hassmann Dover, NJ 07801-5001

No. Of Copies	Organization
1	Commander USA Concepts Analysis Agency ATTN: D. Hardison 8120 Woodmont Avenue Bethesda, MD 20014-2797
1	US Army Ballistic Missile Defense Systems Command Advanced Technology Center P.O. Box 1500 Huntsville, AL 35807-3801
1	Commander US Army Materiel Command ATTN: AMCDE-DW 5001 Eisenhower Avenue Alexandria, VA 22333-5001
1	Cannon Artillery Weapons System, ARDEC, AMCCOM ATTN: AMCPM-CWW Dover, NJ 07801-5001
1	Cannon Artillery Weapons System, ARDEC, AMCCOM ATTN: AMCPM-CWA R. DeKleine Dover, NJ 07801-5001
1	Project Manager Munition Production Base Modernization and Expansion ATTN: AMCPM-PBM-EL, Laibson Dover, NJ 07801-5001

No. Of Copies	Organization	No. Of Copies	Organization
1	Project Manager Tank Main Armament Systems ATTN: AMCPM-TMA, K. Russell Dover, NJ 07801-5001	1	Project Manager Tank Main Armament Systems ATTN: AMCPM-TMA-105 Dover, NJ 07801-5001
1	Project Manager Tank Main Armament Systems ATTN: AMCPM-TMA-120 Dover, NJ 07801-5001	1	Chairman DOD Explosives Safety Board Room 856-C, Hoffman Bldg. 1 2461 Eisenhower Avenue Alexandria, VA 22331-999
1	Commander US Army Material Command ATTN: AMCPM-GCM-WF 5001 Eisenhower Avenue Alexandria, VA 22333-5001		
1	Commander US Army ARDEC, AMCCOM ATTN: SMCAR-TSS Picatinny Arsenal, NJ 07806-5000		
1	Commander US Army ARDEC, AMCCOM ATTN: SMCAR-LC LTC N. Baron Picatinny Arsenal, NJ 07806-5000	1	Commander US Army, ARDEC, AMCCOM ATTN: SMCAR-LCA A. Beardell Picatinny Arsenal, NJ 07806-5000
1	Commander US Army, ARDEC, AMCCOM ATTN: SMCAR-LCA D. Downs Picatinny Arsenal, NJ 07806-5000	1	Commander US Army, ARDEC, AMCCOM ATTN: SMCAR-LCA S. Einstein Picatinny Arsenal, NJ 07806-5000

No. Of Copies	Organization
1	Commander US Army, ARDEC, AMCCOM ATTN: SMCAR-LCA S. Westley Picatinny Arsenal, NJ 07806-5000
1	Commander US Army, ARDEC, AMCCOM ATTN: SMCAR-LCA C. Roller Picatinny Arsenal, NJ 07806-5000
1	Commander US Army, ARDEC, AMCCOM ATTN: SMCAR-LCB-I D. Spring Picatinny Arsenal, NJ 07806-5000
1	Commander US Army, ARDEC, AMCCOM ATTN: SMCAR-LCS Picatinny Arsenal, NJ 07806-5000
1	Commander US Army ARDEC, AMCCOM ATTN: SMCAR-LCU-CT R. Davitt Picatinny Arsenal, NJ 07806-5000
1	Commander US Army, ARDEC, AMCCOM ATTN: SMCAR-LCW-A M. Salsbury Picatinny Arsenal, NJ 07806-5000
1	Commander US Army, ARDEC, AMCCOM ATTN: SMCAR-SCA B. Brodman Picatinny Arsenal, NJ 07806-5000

No. Of Copies	Organization
1	Commander US Army, ARDEC, AMCCOM ATTN: SMCAR-LCA S. Bernstein Picatinny Arsenal, NJ 07806-5000
1	Commander US Army, ARDEC, AMCCOM ATTN: SMCAR-LCA J. Rutkowski Picatinny Arsenal, NJ 07806-5000
1	Commander US Army, ARDEC, AMCCOM ATTN: SMCAR-LCE Picatinny Arsenal, NJ 07806-5000
1	Commander US Army ARDEC, AMCCOM ATTN: SMCAR-LCU-CT E. Barrieres Picatinny Arsenal, NJ 07806-5000
1	Commander US Army, ARDEC, AMCCOM ATTN: SMCAR-LCU-CV C. Mandala Picatinny Arsenal, NJ 07806-5000
1	Commander US Army, ARDEC, AMCCOM ATTN: SMCAR-SCA L. Stiefel Picatinny Arsenal, NJ 07806-5000

No. Of Copies	Organization
1	Commander US Army TSARCOM 4300 Goodfellow Blvd. St. Louis, MO 63120-1702
1	Commander US Army Missile and Space Intelligence Center ATTN: AIAMS-YDL Redstone Arsenal, AL 35898-5500
1	Commandant US Army Aviation School ATTN: Aviation Agency Fort Rucker, AL 36360
1	Commander US Army Tank Automotive Command ATTN: AMSTA-CG Warren, MI 48090
1	Project Manager M-60 Tank Development ATTN: AMCPM-M60TD Warren, MI 48092-2498

No. Of Copies	Organization
1	Commander US Army Harry Diamond Lab ATTN: DELHD-TA-L 2800 Powder Mill Road Adelphi, MD 20783-1145
1	Commander ERADCOM Technical Library ATTN: DELSD-L (Report Section) Fort Monmouth, NJ 07703-5301
1	President US Army Armor & Engineer Board ATTN: ATZK-AD-S Fort Knox, KY 40121-5200

No. Of Copies	Organization	No. Of Copies	Organization
1	Commander U.S. Army Training and Doctrine Command ATTN: ATCD-MA/MAJ Williams Fort Monroe, VA 23651	2	Commander US Materials Technology Laboratory ATTN: SLCMT-ATL Watertown, MA 02172-0001
1	Project Manager Improved TOW Vehicle ATTN: AMCPM-ITV US Army Tank Automotive Command Warren, MI 48397-5000	2	Program Manager M1 Abrams Tank System ATTN: AMCPM-GMC-SA, T. Dean Warren, MI 48092-2498
1	Project Manager Fighting Vehicle Systems ATTN: AMCPM-FVS Warren, MI 48092-2498		
1	Office of Naval Research ATTN: Code 473, R.S. Miller 800 N. Quincy Street Arlington, VA 22217-9999	1	Commandant US Army Command and General Staff College Fort Leavenworth, KS 66027
1	Commandant US Army Special Warfare School ATTN: Rev & Tng Lit Div Fort Bragg, NC 28307	1	Commander Radford Army Ammunition Plant ATTN: SMCRA-QA/HI LIB Radford, VA 24141-0298
1	Commander US Army Foreign Science & Technology Center ATTN: AMXST-MC-3 Charlottesville, VA 22901-5396	1	Commander US Army Research Office ATTN: Tech Library P.O. Box 12211 Research Triangle Park, NC 27709-2211
1	Commander US Army Belvoir Research & Development Center ATTN: STRBE-WC Fort Belvoir, VA 22060-5606	1	Commander US Army Logistics Mgmt Ctr Defense Logistics Studies Fort Lee, VA 23801

No. Of Copies	Organization
1	President US Army Artillery Board Ft. Sill, OK 73503-5600
1	Commander Naval Sea Systems Command ATTN: SEA 62R Washington, DC 20362-5101
1	Commander Naval Air Systems Command ATTN: AIR-954-Tech Lib Washington, DC 20360
1	Naval Research Lab Tech Library Washington, DC 20375
1	Commander Naval Surface Weapons Center ATTN: Code G33, W. Burrell Dahlgren, VA 22448-5000
1	Commander Naval Surface Weapons Center ATTN: Code G23, D. McClure Dahlgren, VA 22448-5000
1	Commander US Naval Surface Weapons Center ATTN: J.P. Consaga Indian Head, MD 20640-5000

No. Of Copies	Organization
3	Commandant US Army Armor School ATTN: ATZK-CD-MS M. Falkovitch Armor Agency Fort Knox, KY 40121-5215
1	Commander Naval Sea Systems Command ATTN: SEA 64 Washington, DC 20362-5101
1	Assistant Secretary of the Navy (R, E, and S) ATTN: R. Reichenbach Room 5E787 Pentagon Bldg. Washington, DC 20350
1	Commander Naval Surface Weapons Center ATTN: Code G33, J.L. East Dahlgren, VA 22448-5000
1	Commander Naval Surface Weapons Center ATTN: Code G33, J. Johndrow Dahlgren, VA 22448-5000
1	Commander Naval Surface Weapons Center ATTN: Code DX-21 Tech Lib Dahlgren, VA 22448-5000
1	Commander US Naval Surface Weapons Center ATTN: C. Gotzmer Indian Head, MD 20640-5000

No. Of Copies	Organization	No. Of Copies	Organization
1	Commander Naval Surface Weapons Center ATTN: S. Jacobs/Code 240 Silver Springs, MD 20903-5000	1	Commander Naval Surface Weapons Center ATTN: Code 730 Silver Springs, MD 20903-5000
1	Commander Naval Surface Weapons Center ATTN: K. Kim/Code R-13 Silver Springs, MD 20903-5000	1	Commander Naval Surface Weapons Center ATTN: R. Bernecker Silver Springs, MD 20903-5000
1	Commanding Officer Naval Underwater Systems Center Energy Conversion Dept. ATTN: Code 5B331, R.S. Lazar Newport, RI 02840	1	Commanding Officer Naval Underwater Systems Center Energy Conversion Dept. ATTN: Tech Library Newport, RI 02840
1	Commander Naval Weapons Center ATTN: Code 388, R.L. Derr Info. Sci. Div. China Lake, CA 93555-6001	1	Commander Naval Weapons Center ATTN: Code 388, C.F. Price Info. Sci. Div. China Lake, CA 93555-6001
1	Commander Naval Weapons Center ATTN: Code 388, T. Boggs Info. Sci. Div. China Lake, CA 93555-6001	2	Commandant US Army Field Artillery Center & School ATTN: ATSF-CO-MW, B. Willis Ft. Sill, OK 73503-5600
1	Commander US Army Development and Employment Agency ATTN: MODE-TED-SAB Fort Lewis, WA 98433-5099	1	Commander Naval Ordnance Station ATTN: P.L. Stang Indian Head, MD 20640-5000
1	Commander Naval Ordnance Station ATTN: J. Birkett Indian Head, MD 20640-5000	1	Commander Naval Ordnance Station ATTN: L. Torreyson Indian Head, MD 20640-5000

No. Of Copies	Organization	No. Of Copies	Organization
1	Commander Naval Ordnance Station ATTN: T.C. Smith Indian Head, MD 20640-5000	1	Commander Naval Ordnance Station ATTN: D. Brooks Indian Head, MD 20640-5000
1	Commander Naval Ordnance Station ATTN: Tech Library Indian Head, MD 20640-5000	1	AFSC/SDOA Andrews AFB, MD 20334
1	AFRPL/DY, Stop 24 ATTN: J. Levine/DYCR Edwards AFB, CA 93523-5000	1	AFRPL/DY, Stop 24 ATTN: R. Corley/DYC Edwards AFB, CA 93523-5000
1	AFRPL/DY, Stop 24 ATTN: D. Williams/DYCC Edwards AFB, CA 93523-5000	1	AFRPL/TSTL (Tech Library) Stop 24 Edwards AFB, CA 93523-5000
1	AFATL/DLYV Eglin AFB, FL 32542-5000	1	AFATL/DLXP Eglin AFB, FL 32542-5000
1	AFATL/DLJE Eglin AFB, FL 32542-5000	2	Superintendent Naval Postgraduate School Department of Mechanical Engineering Monterey, CA 93943-5100
		1	NASA/Lyndon B. Johnson Space Center ATTN: NHS-22, Library Section Houston, TX 77054

No. Of Copies	Organization	No. Of Copies	Organization
		1	AAI Corporation ATTN: J. Frankle P.O. Box 6767 Baltimore, MD 21204
1	Aerojet Ordnance Company ATTN: D. Thatcher 2521 Michelle Drive Tustin, CA 92680-7014		
1	Program Manager AFOSR Directorate of Aerospace Sciences ATTN: L.H. Caveny Bolling AFB, DC 20332-0001	2	Calspan Corporation ATTN: C. Morphy P.O. Box 400 Buffalo, NY 14225-0400
10	Central Intelligence Agency Office of Central Reference Dissemination Branch Room GE-47 HQS Washington, DC 20505	1	General Electric Company Armament Systems Dept. ATTN: M.J. Bulman, Room 1311 128 Lakeside Avenue Burlington, VT 05401-4985
1	IITRI ATTN: M.J. Klein 10 W. 35th Street Chicago, IL 60616-3799	1	Hercules, Inc. Allegheny Ballistics Laboratory ATTN: R.B. Miller P.O. Box 210 Cumberland, MD 21501-0210
1	Aerojet Solid Propulsion Co. ATTN: P. Micheli Sacramento, CA 95813	1	Atlantic Research Corporation ATTN: M.K. King 5390 Cheorokee Avenue Alexandria, VA 22312-2302
1	Honeywell, Inc. ATTN: C. Hargraves 7225 Northland Dr. Minneapolis, MN	1	Lawrence Livermore National Laboratory ATTN: L-355, A. Buckingham P.O. Box 808 Livermore, CA 94550-0622

No. Of Copies	Organization	No. Of Copies	Organization
1	Lawrence Livermore National Laboratory ATTN: L-355, M. Finger P.O. Box 808 Livermore, CA 94550-0622	1	Lawrence Livermore National Laboratory ATTN: L-324 M. Constantino P.O. Box 808 Livermore, CA 94550-0622
1	Olin Corporation Badger Army Ammunition Plant ATTN: R.J. Thiede Baraboo, WI 53913	1	Olin Corporation Smokeless Powder Operations ATTN: D.C. Mann P.O. Box 222 St. Marks, FL 32355-0222
1	Paul Gough Associates ATTN: P.S. Gough 1048 South Street Portsmouth, NH 03801-5423	1	Hercules, Inc. Radford Army Ammunition Plant ATTN: J. Pierce Radford, VA 24141-0299
1	AVCO Everett Rsch Lab ATTN: D. Stickler 2385 Revere Beach Parkway Everett, MA 02149-5936	1	Princeton Combustion Research Lab., Inc. ATTN: M. Summerfield 475 US Highway One Monmouth Junction, NJ 08852-9650
1	Rockwell International Rocketdyne Division ATTN: BA08 J.E. Flanagan 6633 Canoga Avenue Canoga Park, CA 91303-2703	1	Science Applications, Inc. ATTN: R.B. Edelman 23146 Cumorah Crest Drive Woodland Hills, CA 91364-3710
1	Rockwell International Rocketdyne Division ATTN: BA08 J. Gray 6633 Canoga Avenue Canoga Park, CA 91303-2703	1	Thiokol Corporation Huntsville Division ATTN: D. Flanigan Huntsville, AL 35807
1	Thiokol Corporation Huntsville Division ATTN: R. Glick Huntsville, AL 35807	1	Thiokol Corporation Huntsville Division ATTN: Tech Library Huntsville, AL 35807

No. Of Copies	Organization	No. Of Copies	Organization
1	Scientific Research Assoc., Inc. ATTN: H. McDonald P.O. Box 498 Glastonbury, CT 06033-0498	1	Veritay Technology, Inc. ATTN: E. Fisher 4845 Millersport Hwy. P.O. Box 305 East Amherst, NY 14051-0305
1	Physics International Company ATTN: Library 2700 Merced Street San Leandro, CA 94577-5602	1	Physics International Company ATTN: H. Wayne Wampler 2700 Merced Street San Leandro, CA 94577-5602
1	United Technologies Chemical Systems Division ATTN: Tech Library P.O. Box 358 Sunnyvale, CA 94086-9998	1	Universal Propulsion Company ATTN: H. J. McSpadden Black Canyon Stage 1 Box 1140 Phoenix, AZ 85029
1	Battelle Memorial Institute ATTN: Tech Library 505 King Avenue Columbus, OH 43201-2693	1	Brigham Young University Dept of Chemical Engineering ATTN: M. Beckstead Provo, UT 84601
1	California Institute of Tech 204 Karman Lab Main Stop 301-46 ATTN: F.E.C. Culick 1201 E. California Street Pasadena, CA 91109	1	Thiokol Corporation Elkton Division ATTN: R. Biddle P.O. Box 241 Elkton, MD 21921-0241
1	Thiokol Corporation Elkton Division ATTN: Tech Lib. P.O. Box 241 Elkton, MD 21921-0241	1	University o Massachusetts Dept. of Mechanical Engineering ATTN: K. Jakus Amherst, MA 01002-0014
1	University of Minnesota Dept of Mechanical Engineering ATTN: E. Fletcher Minneapolis, MN 55414-3368	1	Case Western Reserve University Division of Aerospace Sciences ATTN: J. Tien Cleveland, OH 44135

No. Of Copies	Organization	No. Of Copies	Organization
1	Georgia Institute of Tech School of Aerospace Eng. ATTN: B.T. Zinn Atlanta, GA 30332	1	Georgia Institute of Tech School of Aerospace Eng. ATTN: E. Price Atlanta, GA 30332
1	Georgia Institute of Tech School of Aerospace Eng. ATTN: W.C. Strahle Atlanta, GA 30332	1	Institute of Gas Technology ATTN: D. Gidaspow 3424 S. State Street Chicago, IL 60616-3896
1	Johns Hopkins University Applied Physics Laboratory Chemical Propulsion Information Agency ATTN: T. Christian Johns Hopkins Road Laurel, MD 20707-0690	1	California Institute of Tech Jet Propulsion Laboratory ATTN: L.D. Strand 4800 Oak Grove Drive Pasadena, CA 91109-8099
1	University of Illinois Dept of Mech/Indust Engr ATTN: H. Krier 144 MEB; 1206 N. Green St. Urbana, IL 61801-2978	1	University of Southern California Mechanical Engineering Dept. ATTN: OHE200, M. Gerstein Los Angeles, CA 90089-5199
1	University of Utah Dept of Chemical Engineering ATTN: A. Baer Salt Lake City, UT 84112-1194	1	University of Utah Dept of Chemical Engineering ATTN: G. Flandro Salt Lake City, UT 84112-1194
1	Washington State University Dept of Mechanical Engineering ATTN: C.T. Crowe Pullman, WA 99163-5201	1	Rensselaer Polytechnica Inst. Department of Mathematics Troy, NY 12181
1	Massachusetts Institute of Technology Dept of Mechanical Engineering ATTN: T. Toong 77 Massachusetts Ave Cambridge, MA 02139-4307	1	G.M. Faeth Pennsylvania State University Applied Research Laboratory University Park, PA 16802-7501

No. Of Copies	Organization
1	Pennsylvania State University Dept of Mech. Engineering ATTN: K. Kuo University Park, PA 16802-7501
1	SRI International Propulsion Sciences Division ATTN: Tech Library 333 Ravenswood Ave Menlo Park, CA 94025-3493
1	Rutgers University Dept of Mechanical and Aerospace Engineering ATTN: S. Temkin University Heights Campus New Brunswick, NJ 08903

No. Of Copies	Organization
1	Purdue University School of Mechanical Engineering ATTN: J.R. Osborn TSPC Chaffee Hall West Lafayette, IN 47907-1199
1	Stevens Institute of Technology Davidson Laboratory ATTN: R. McAlevy, III Castle Point Station Hoboken, NJ 07030-5907